Evaluation of small amounts of samples. One malignant pleural effusion sample and 17 biopsy specimens, including TBB (n=13), lymph node biopsy (n=2), needle biopsy (n=2), and 22 surgical specimens, were used for mutation analyses (Table III). Mutations were detected in 7 surgical samples (30.4%), while of the 18 non-surgical specimens 11 (61.1%) showed mutations. In order to validate these results, mutation analyses were also performed on three surgical specimens, for which the corresponding non-surgical specimens had not shown any mutations, and on an autopsy specimen whose lymph node biopsy had revealed a deletion mutation in exon 19. Identical results were obtained for both the surgical and non-surgical specimens.

Discussion

The aim of the present study was to identify predictive factors for gefitinib sensitivity and patient prognosis as well as risk factors for adverse events associated with gefitinib therapy. Female gender and never having smoked are newly identified as candidate risk factors for stomatitis. Stomatitis is a common adverse event of gefitinib therapy and often impairs quality of life (QOL), and both female gender and non-smoking are also predictive factors for the effect of gefitinib (17, 18).

In the present study, EGFR mutations were identified in 18 of 44 patients (40.9%). Although the mutation rate established here was similar to the previous reports from eastern Asia (17, 18), the overall mutation rate in this study was slightly higher (18.9% to 47.6%; mean 36.0%), whereas in clinically responsive cases it was relatively low (52.4% to 82.8%; mean 74.4%) compared to those previous reported (4, 5, 7-9, 11-14). Possible reasons for the lower mutation rate in clinically responsive cases may include (i) other factors defining gefitinib sensitivity, (ii) the remaining tumor acquired an EGFR mutation after we had obtained specimens, and (iii) the small number of cases analyzed influenced the result. Other factors defining gefinitib sensitivity could include increased EGFR or HER2 gene copy number and protein phosphorylation of Akt, PTEN, ERK1/2, or STAT5 (19-27). Increased copy number of the HER3 or 4 genes should be also evaluated because their products can form heterodimers with EGFR, whilst protein expression or phosphorylation in signalling pathways other than Akt, PTEN, ERK1/2 and STAT5 might be important. Small biopsy specimens might not have faithfully reflected the major characteristics of individual tumors, in that the proportion of tumor cells harboring EGFR mutations within analyzed specimens may have been so low that insufficient cells with mutations were included, in addition, some reports showed that the detection rate of EGFR mutation by new methods seemed to be superior to that by direct sequencing methods (28, 29). Whilst the direct sequencing method was the only one used in the present study, the differences we found are unlikely due to specimen size as because the feasibility of using small specimens for EGFR mutational analysis was evaluated, and surgical materials and the corresponding non-surgical and small specimens revealed consistent results in mutation analyses. Furthermore, the detection efficiency of EGFR mutations in small specimens such as biopsy fragments or cells recovered from pleural effusion was comparable to that in surgical materials. However, it might be necessary to examine more cases because the feasibility was evaluated for 4 pairs and only one mutation case could be verified.

The group of patients with EGFR mutations experienced better TTP and OS. However, this difference was not statistically significant. This could also be explained by the same factors defining gefitinib sensitivity as those described in possible reasons for the lower mutation rate in clinically responsive cases. Another explanation may be that the sample of patients was enriched with gefitinib-responsive cases because of the retrospective nature of the study. Because clinical responses would yield significant differences in OS as well as in TTP, and no mutations were found in any cases but one refractory to gefitinib, larger-scale mutation analysis eliminating "selectivity bias" could lead to statistical significance in TTP and OS. A third explanation may be that analytical or technical limitations, such as employing direct sequencing or using paraffin-embedded tissues may have affected the mutation detection rate; the development of new analytical methods aims to overcome such limitations (28, 29).

Conclusion

We have identified certain clinicopathological characteristics as well as EGFR mutations which can be either predictive factors for gefitinib sensitivity or risk factors for adverse events associated with gefitinib therapy. EGFR mutations could be identified from biopsy or cytology specimens in patients with advanced NSCLC. These data might contribute to establishing optimum gefitinib therapy for NSCLC patients, especially at advanced stages.

Acknowledgements

We gratefully acknowledge financial support from the AstraZeneca Research Grant 2005.

References

1 Fukuoka M, Yano S, Giaccone G, Tamura T, Nakagawa K, Douillard JY, Nishiwaki Y, Vansteenkiste J, Kudoh S, Rischin D, Eek R, Horai T, Noda K, Takata I, Smit E, Averbuch S, Macleod A, Feyereislova A, Dong RP and Baselga J: Multi-institutional randomized phase II trial of gefitinib for previously treated patients with advanced non-small-cell lung cancer (The IDEAL 1 Trial) J Clin Oncol *21*: 2237-2246, 2003.

2 Lynch TJ, Bell DW, Sordella R, Gurubhagavatula S, Okimoto RA, Brannigan BW, Harris PL, Haserlat SM, Supko JG, Haluska FG, Louis DN, Christiani DC, Settleman J and Haber DA: Activating mutations in the epidermal growth factor receptor underlying responsiveness of non-small-cell lung cancer to gefitinib. N Engl J Med *350*: 2129-2139, 2004.

3 Paez JG, Janne PA, Lee JC, Tracy S, Greulich H, Gabriel S, Herman P, Kaye FJ, Lindeman N, Boggon TJ, Naoki K, Sasaki H, Fujii Y, Eck MJ, Sellers WR, Johnson BE and Meyerson M: EGFR mutations in lung cancer: correlation with clinical response to gefitinib therapy. Science *304*: 1497-1500, 2004.

4 Kosaka T, Yatabe Y, Endoh H, Kuwano H, Takahashi T and Mitsudomi T: Mutations of the epidermal growth factor receptor gene in lung cancer: biological and clinical implications. Cancer Res *64*: 8919-8923, 2004.

5 Huang SF, Liu HP, Li LH, Ku YC, Fu YN, Tsai HY, Chen YT, Lin YF, Chang WC, Kuo HP, Wu YC, Chen YR and Tsai SF: High frequency of epidermal growth factor receptor mutations with complex patterns in non-small cell lung cancers related to gefitinib responsiveness in Taiwan. Clin Cancer Res *10*: 8195-8203, 2004.

6 Tokumo M, Toyooka S, Kiura K, Shigematsu H, Tomii K, Aoe M, Ichimura K, Tsuda T, Yano M, Tsukuda K, Tabata M, Ueoka H, Tanimoto M, Date H, Gazdar AF and Shimizu N: The relationship between epidermal growth factor receptor mutations and clinicopathologic features in non-small cell lung cancers. Clin Cancer Res *11*: 1167-1173, 2005.

7 Mitsudomi T, Kosaka T, Endoh H, Horio Y, Hida T, Mori S, Hatooka S, Shinoda M, Takahashi T and Yatabe Y: Mutations of the epidermal growth factor receptor gene predict prolonged survival after gefitinib treatment in patients with non-small-cell lung cancer with postoperative recurrence. J Clin Oncol *23*: 2513-2520, 2005.

8 Han SW, Kim TY, Hwang PG, Jeong S, Kim J, Choi IS, Oh DY, Kim JH, Kim DW, Chung DH, Im SA, Kim YT, Lee JS, Heo DS, Bang YJ and Kim NK: Predictive and prognostic impact of epidermal growth factor receptor mutation in non-small-cell lung cancer patients treated with gefitinib. J Clin Oncol *23*: 2493-2501, 2005.

9 Kim KS, Jeong JY, Kim YC, Na KJ, Kim YH, Ahn SJ, Baek SM, Park CS, Park CM, Kim YI, Lim SC and Park KO: Predictors of the response to gefitinib in refractory non-small cell lung cancer. Clin Cancer Res *11*: 2244-2251, 2005.

10 Bell DW, Lynch TJ, Haserlat SM, Harris PL, Okimoto RA, Brannigan BW, Sgroi DC, Muir B, Riemenschneider MJ, Iacona RB, Krebs AD, Johnson DH, Giaccone G, Herbst RS, Manegold C, Fukuoka M, Kris MG, Baselga J, Ochs JS and Haber DA: Epidermal growth factor receptor mutations and gene amplification in non-small-cell lung cancer: molecular analysis of the IDEAL/INTACT gefitinib trials. J Clin Oncol *23*: 8081-8092, 2005.

11 Taron M, Ichinose Y, Rosell R, Mok T, Massuti B, Zamora L, Mate JL, Manegold C, Ono M, Queralt C, Jahan T, Sanchez JJ, Sanchez-Ronco M, Hsue V, Jablons D, Sanchez JM and Moran T: Activating mutations in the tyrosine kinase domain of the epidermal growth factor receptor are associated with improved survival in gefitinib-treated chemorefractory lung adenocarcinomas. Clin Cancer Res *11*: 5878-5885, 2005.

12 Tomizawa Y, Iijima H, Sunaga N, Sato K, Takise A, Otani Y, Tanaka S, Suga T, Saito R, Ishizuka T, Dobashi K, Minna JD, Nakajima T and Mori M: Clinicopathologic significance of the mutations of the epidermal growth factor receptor gene in patients with non-small cell lung cancer. Clin Cancer Res *11*: 6816-6822, 2005.

13 Uramoto H, Sugio K, Oyama T, Ono K, Sugaya M, Yoshimatsu T, Hanagiri T, Morita M and Yasumoto K: Epidermal growth factor receptor mutations are associated with gefitinib sensitivity in non-small cell lung cancer in Japanese. Lung Cancer *51*: 71-77, 2006.

14 Sasaki H, Endo K, Mizuno K, Yano M, Fukai I, Yamakawa Y and Fujii Y: EGFR mutation status and prognosis for gefitinib treatment in Japanese lung cancer. Lung Cancer *51*: 135-136, 2006.

15 Shih JY, Gow CH, Yu CJ, Yang CH, Chang YL, Tsai MF, Hsu YC, Chen KY, Su WP and Yang PC: Epidermal growth factor receptor mutations in needle biopsy/aspiration samples predict response to gefitinib therapy and survival of patients with advanced nonsmall cell lung cancer. Int J Cancer 2005.

16 Kobayashi S, Boggon TJ, Dayaram T, Janne PA, Kocher O, Meyerson M, Johnson BE, Eck MJ, Tenen DG and Halmos B: EGFR mutation and resistance of non-small-cell lung cancer to gefitinib. N Engl J Med *352*: 786-792, 2005.

17 Hotta K, Kiura K, Tabata M, Harita S, Gemba K, Yonei T, Bessho A, Maeda T, Moritaka T, Shibayama T, Matsuo K, Kato K, Kanehiro A, Tanimoto Y, Ueoka H and Tanimoto M: Interstitial lung disease in Japanese patients with non-small cell lung cancer receiving gefitinib: an analysis of risk factors and treatment outcomes in Okayama Lung Cancer Study Group. Cancer J *11*: 417-424, 2005.

18 Takano T, Ohe Y, Kusumoto M, Tateishi U, Yamamoto S, Nokihara H, Yamamoto N, Sekine I, Kunitoh H, Tamura T, Kodama T and Saijo N: Risk factors for interstitial lung disease and predictive factors for tumor response in patients with advanced non-small cell lung cancer treated with gefitinib. Lung Cancer *45*: 93-104, 2004.

19 She QB, Solit D, Basso A and Moasser MM: Resistance to gefitinib in PTEN-null HER-overexpressing tumor cells can be overcome through restoration of PTEN function or pharmacologic modulation of constitutive phosphatidylinositol 3'-kinase/Akt pathway signaling. Clin Cancer Res *9*: 4340-4346, 2003.

20 Kokubo Y, Gemma A, Noro R, Seike M, Kataoka K, Matsuda K, Okano T, Minegishi Y, Yoshimura A, Shibuya M and Kudoh S: Reduction of PTEN protein and loss of epidermal growth factor receptor gene mutation in lung cancer with natural resistance to gefitinib (IRESSA). Br J Cancer *92*: 1711-1719, 2005.

21 Cappuzzo F, Hirsch FR, Rossi E, Bartolini S, Ceresoli GL, Bemis L, Haney J, Witta S, Danenberg K, Domenichini I, Ludovini V, Magrini E, Gregorc V, Doglioni C, Sidoni A, Tonato M, Franklin WA, Crino L, Bunn PA Jr and Varella-Garcia M: Epidermal growth factor receptor gene and protein and gefitinib sensitivity in non-small-cell lung cancer. J Natl Cancer Inst *97*: 643-655, 2005.

22 Takano T, Ohe Y, Sakamoto H, Tsuta K, Matsuno Y, Tateishi U, Yamamoto S, Nokihara H, Yamamoto N, Sekine I, Kunitoh H, Shibata T, Sakiyama T, Yoshida T and Tamura T: Epidermal growth factor receptor gene mutations and increased copy numbers predict gefitinib sensitivity in patients with recurrent non-small-cell lung cancer. J Clin Oncol *23*: 6829-6837, 2005.

23 Hirsch FR, Varella-Garcia M, McCoy J, West H, Xavier AC, Gumerlock P, Bunn PA Jr, Franklin WA, Crowley J and Gandara DR: Increased epidermal growth factor receptor gene copy number detected by fluorescence *in situ* hybridization associates with increased sensitivity to gefitinib in patients with bronchioloalveolar carcinoma subtypes: a Southwest Oncology Group Study. J Clin Oncol *23*: 6838-6845, 2005.

24 Cappuzzo F, Varella-Garcia M, Shigematsu H, Domenichini I, Bartolini S, Ceresoli GL, Rossi E, Ludovini V, Gregorc V, Toschi L, Franklin WA, Crino L, Gazdar AF, Bunn PA Jr and Hirsch FR: Increased HER2 gene copy number is associated with response to gefitinib therapy in epidermal growth factor receptor-positive non-small-cell lung cancer patients. J Clin Oncol *23*: 5007-5018, 2005.

25 Cappuzzo F, Magrini E, Ceresoli GL, Bartolini S, Rossi E, Ludovini V, Gregorc V, Ligorio C, Cancellieri A, Damiani S, Spreafico A, Paties CT, Lombardo L, Calandri C, Bellezza G, Tonato M and Crino L: Akt phosphorylation and gefitinib efficacy in patients with advanced non-small-cell lung cancer. J Natl Cancer Inst *96*: 1133-1141, 2004.

26 Amann J, Kalyankrishna S, Massion PP, Ohm JE, Girard L, Shigematsu H, Peyton M, Juroske D, Huang Y, Stuart Salmon J, Kim YH, Pollack JR, Yanagisawa K, Gazdar A, Minna JD, Kurie JM and Carbone DP: Aberrant epidermal growth factor receptor signaling and enhanced sensitivity to EGFR inhibitors in lung cancer. Cancer Res *65*: 226-35, 2005.

27 Sordella R, Bell DW, Haber DA and Settleman J: Gefitinib-sensitizing EGFR mutations in lung cancer activate anti-apoptotic pathways. Science *305*: 1163-1167, 2004.

28 Nagai Y, Miyazawa H, Huqun, Tanaka T, Udagawa K, Kato M, Fukuyama S, Yokote A, Kobayashi K, Kanazawa M and Hagiwara K: Genetic heterogeneity of the epidermal growth factor receptor in non-small cell lung cancer cell lines revealed by a rapid and sensitive detection system, the peptide nucleic acid-locked nucleic acid PCR clamp. Cancer Res *65*: 7276-7282, 2005.

29 Endo K, Konishi A, Sasaki H, Takada M, Tanaka H, Okumura M, Kawahara M, Sugiura H, Kuwabara Y, Fukai I, Matsumura A, Yano M, Kobayashi Y, Mizuno K, Haneda H, Suzuki E, Iuchi K and Fujii Y: Epidermal growth factor receptor gene mutation in non-small cell lung cancer using highly sensitive and fast TaqMan PCR assay. Lung Cancer *50*: 375-384, 2005.

Received August 29, 2006
Accepted October 4, 2006

ANTICANCER RESEARCH

International Journal of Cancer Research and Treatment

ISSN: 0250-7005

October 4, 2006

Dr. Nobuyuki Koyama

Re: Your manuscript No. **7441-K** entitled **«The Characterization of Gefitinib Sensitivity...»**

Dear Dr

Referring to your above manuscript for publication in AR, please allow us to use this form letter in reply:

1. *Referee's recommendations:*
   - ■ Urgent to be published immediately.
   - □ Accepted in the presented form.
   - □ Accepted with minor changes.
   - ■ Accepted with grammatical or language corrections.
   - ■ Remarks: **1) Reference No 15 is incomplete 2) Page 4 of proofs reference missing: The therapeutic effect of gefitinib was determined according to the Response Evaluation Criteria in Solid Tumors (RECIST).**

2. *Excess page charges.*
   - ■ Your article has approx. **7** printed pages and is in excess of the allotted number by approx. **3** printed pages. The charges are EURO € **190** per excess page, totalling EURO € **570**
     We ask you to confirm acceptance of these charges.
   - □ Your article includes pages with color figures. The charges are EURO € per color page, totalling EURO €
   - ■ Our invoice is sent by air mail to the corresponding author.

3. ■ Your article will appear in Volume **26**, Issue No. **6, 2006**

4. ■ Please order your reprints now. This will facilitate our prompt planning of future issues and rapid publication of your article. Reprints will be delivered by air mail within one month from publication.

We would appreciate your prompt reply.
With many thanks,
Yours sincerely,

J.G. Delinassios
Managing Editor

EDITORIAL OFFICE: INTERNATIONAL INSTITUTE OF ANTICANCER RESEARCH
1st km Kapandritiou - Kalamou Rd., Kapandriti, P.O.B. 22, Attiki 19014, Greece. Tel.: 0030-22950-52945;
Tel & Fax:0030-22950-53389; e-mail: journals@iiar-anticancer.org

ANTICANCER RESEARCH
International Journal of Cancer Research and Treatment

ISSN: 0250-7005

Editorial Office: International Institute of Anticancer Research,
1st km Kapandritiou - Kalamou Rd., Kapandriti, P.O.B. 22, Attiki 19014, Greece
Fax:0030-22950-53389;Tel.: 0030-22950-52945; e-mail: journals@iiar-anticancer.org

Please type or print the requested information on the reprint order form and return it to the Editorial Office by fax or e-mail.
Reprints must be paid for in advance.
If your paper is subject to charges for excess pages or color plates, please add these charges to the payment for reprints.
The reprints are not to be sold.

PRICE LIST FOR REPRINTS WITHOUT COVER

	Number of copies requested									
Page length	100	200	300	400	500	1000	1500	2000	3000	5000
1-4pp EURO	335	387	438	503	554	851	1135	1470	2038	3225
5-8	438	503	580	645	722	1083	1445	1832	2554	4012
9-12	554	619	709	787	877	1341	1780	2219	3096	4824
13-16	709	787	890	993	1096	1625	2141	2657	3676	5715
17-20	838	929	1032	1148	1277	1883	2451	3044	4244	6527

For reprints with cover: Please add EURO 140.00 per 100 copies.
Postage: Please add 4% on the above prices.

Reprint Order Form

Of my paper No. **7441-K** comprising **7** printed pages, entitled «**The Characterization of Gefitinib Sensitivity...**»
accepted for publication in ANTICANCER RESEARCH Vol. **26** No. **6**

☐ I require a total of copies at EURO
☐ I do not require reprints
☐ Please send me a copy of this issue containing my paper at EURO 45.00
☐ Please enter my personal subscription to ANTICANCER RESEARCH at the special Author's price of EURO 400.00 (☐ Year: 2006)
☐ A check for the above amounts payable to J. G. Delinassios, Executive Publisher of Anticancer Research Journal, is enclosed.
☐ Please send an invoice to:

For EC countries: Please give your VAT number:
City and Date: Signature:
Exact postal address:
Tel:
Fax:

Am J Physiol Lung Cell Mol Physiol 290: L194–L199, 2006.
First published August 12, 2005; doi:10.1152/ajplung.00050.2005.

Involvement of the platelet-activating factor receptor in host defense against *Streptococcus pneumoniae* during postinfluenza pneumonia

Koenraad F. van der Sluijs,[1,2,3] Leontine J. R. van Elden,[4] Monique Nijhuis,[4] Rob Schuurman,[4] Sandrine Florquin,[5] Takao Shimizu,[6] Satoshi Ishii,[7] Henk M. Jansen,[2] René Lutter,[2,3] and Tom van der Poll[1]

[1]*Laboratory of Experimental Internal Medicine,* [2]*Department of Pulmonology,* [3]*Laboratory of Experimental Immunology,* [5]*Department of Pathology, Academic Medical Center, University of Amsterdam, Amsterdam;* [4]*Eijkman-Winkler Institute, Department of Virology, University Medical Center, Utrecht, The Netherlands;* [6]*Department of Biochemistry and Molecular Biology, Faculty of Medicine, The University of Tokyo; and* [7]*CREST of Japan Science and Technology Corporation, Tokyo, Japan*

Submitted 26 January 2005; accepted in final form 11 August 2005

van der Sluijs, Koenraad F., Leontine J. R. van Elden, Monique Nijhuis, Rob Schuurman, Sandrine Florquin, Takao Shimizu, Satoshi Ishii, Henk M. Jansen, René Lutter, and Tom van der Poll. Involvement of the platelet-activating factor receptor in host defense against *Streptococcus pneumoniae* during postinfluenza pneumonia. *Am J Physiol Lung Cell Mol Physiol* 290: L194–L199, 2006. First published August 12, 2005; doi:10.1152/ajplung.00050.2005.— Although influenza infection alone may lead to pneumonia, secondary bacterial infections are a much more common cause of pneumonia. *Streptococcus pneumoniae* is the most frequently isolated causative pathogen during postinfluenza pneumonia. Considering that *S. pneumoniae* utilizes the platelet-activating factor receptor (PAFR) to invade the respiratory epithelium and that the PAFR is upregulated during viral infection, we here used PAFR gene-deficient ($PAFR^{-/-}$) mice to determine the role of this receptor during postinfluenza pneumococcal pneumonia. Viral clearance was similar in wild-type and $PAFR^{-/-}$ mice, and influenza virus was completely removed from the lungs at the time mice were inoculated with *S. pneumoniae* (*day 14* after influenza infection). $PAFR^{-/-}$ mice displayed a significantly reduced bacterial outgrowth in their lungs, a diminished dissemination of the infection, and a prolonged survival. Pulmonary levels of IL-10 and KC were significantly lower in $PAFR^{-/-}$ mice, whereas IL-6 and TNF-α were only trendwise lower. These data indicate that the pneumococcus uses the PAFR leading to severe pneumonia in a host previously exposed to influenza A.

virus; bacteria; pneumonia; inflammation

ALTHOUGH INFLUENZA A INFECTION alone may lead to pneumonia, secondary bacterial infections during and shortly after recovery from influenza are much more common causes of pneumonia (12, 28). Bacteria such as *Staphylococcus aureus* and *Haemophilus influenzae* are known to cause postinfluenza pneumonia, but *Streptococcus pneumoniae* is the most prominent pathogen causing secondary bacterial pneumonia in recent decades (28). Primary infection with this pathogen is usually less severe than secondary infection (16). Influenza is known to increase adherence of and subsequent colonization with bacterial respiratory pathogens. Bacteria may adhere to the basal membrane after disruption of the airway epithelial layer by the cytopathic effect of the virus (17) but may also bind to specific receptors in the airway epithelium induced by influenza virus (6, 11). Because the platelet-activating factor receptor (PAFR) has been described to be upregulated during viral infections (10) and since the PAFR is able to bind phosphorylcholine, a cell wall component of *S. pneumoniae* (3, 5, 12), it has been suggested that the PAFR may play a critical role during secondary bacterial pneumonia (11).

The PAFR, a G protein-coupled receptor, is mainly expressed on macrophages, monocytes, neutrophils, and epithelial cells (8, 9, 22, 24). Activation of epithelial cells leads to upregulation of the PAFR at the cell surface, which facilitates colonization and invasion of *S. pneumoniae* (3, 9). A recent study by McCullers and Rehg (11) investigated the potential role of the PAFR in pneumococcal pneumonia following influenza A infection. These authors showed that PAFR blockade during secondary pneumococcal pneumonia does not prevent lethal synergism between influenza virus and *S. pneumoniae* (11). Moreover, administration of the PAFR antagonist CV-6209 resulted in enhanced bacterial outgrowth, even in mice with primary pneumococcal pneumonia (11). These findings contrast with earlier studies reporting that administration of PAFR antagonists reduced pneumococcal outgrowth in rabbits (2, 3). In line, our laboratory recently demonstrated that PAFR gene deficient ($PAFR^{-/-}$) mice display a diminished bacterial outgrowth and a reduced lethality after intranasal infection with *S. pneumoniae* (20). To obtain further insight in the role of the PAFR during secondary bacterial pneumonia, we inoculated $PAFR^{-/-}$ mice and wild-type mice with *S. pneumoniae* on *day 14* after influenza virus infection and studied host defense against primary influenza virus infection and secondary *S. pneumoniae* infection.

MATERIALS AND METHODS

Mice. $PAFR^{-/-}$ mice were generated as described (7) and backcrossed seven times to a C57BL/6 background. Wild-type C57BL/6 mice were obtained from Harlan Sprague-Dawley. Pathogen-free 8-wk-old female C57BL/6 mice and $PAFR^{-/-}$ mice were maintained at biosafety *level 2* during the experiments. All experiments were approved by the Institutional Animal Care and Use Committee of the Academic Medical Center.

Experimental infection protocol. Influenza A/PR/8/34 (VR-95; ATCC, Rockville, MD) was grown on LLC-MK2 cells (RIVM,

Address for reprint requests and other correspondence: K. van der Sluijs, Laboratory of Experimental Immunology, Rm. G1-140, Academic Medical Center, Meibergdreef 9, 1105 AZ, Amsterdam, The Netherlands (e-mail: kvandersluijs@amc.uva.nl).

The costs of publication of this article were defrayed in part by the payment of page charges. The article must therefore be hereby marked "*advertisement*" in accordance with 18 U.S.C. Section 1734 solely to indicate this fact.

Bilthoven, Netherlands). Virus was harvested by a freeze-thaw cycle, followed by centrifugation at 680 *g* for 10 min. Supernatants were stored in aliquots at −80°C. Titration was performed in LLC-MK2 cells to calculate the median tissue culture infective dose ($TCID_{50}$) of the viral stock (18). A noninfected cell culture was used for preparation of the control inoculum. None of the stocks were contaminated by other respiratory viruses, i.e., influenza B; human parainfluenza type 1, 2, 3, 4A, and 4B; Sendai virus; respiratory syncytial virus A and B; rhinovirus; enterovirus; corona virus; and adenovirus; as determined by PCR or cell culture. Viral stock and control stock were diluted just before use in phosphate-buffered saline (PBS, pH 7.4). Primary influenza infection and secondary pneumococcal pneumonia were induced according to previously described methods (30, 31). In brief, mice were anesthetized by inhalation of isoflurane (Abbott Laboratories, Kent, UK) and intranasally inoculated with 10 $TCID_{50}$ influenza (1,400 viral copies) or control inoculum in a final volume of 50 μl of PBS. Pneumococcal pneumonia was induced 14 days after inoculation with influenza or control suspension. *S. pneumoniae serotype 3* (ATCC 6303) was cultured for 16 h at 37°C in 5% CO_2 in Todd Hewitt broth. This suspension was diluted 100 times in fresh medium and grown for 5 h to midlogarithmic phase. Bacteria were harvested by centrifugation at 2,750 *g* for 10 min at 4°C and washed twice with ice-cold saline. After the second wash, bacteria were resuspended in saline and diluted to a concentration of 2×10^5 colony forming units (CFU) per ml, which was verified by plating out 10-fold dilutions onto blood-agar plates. Mice were anesthetized by inhalation with isoflurane and were inoculated with 50 μl of the bacterial suspension (10^4 CFU *S. pneumoniae*).

Determination of PAFR expression in the lungs. The expression of the PAFR in the lungs was determined on *day 8* and *day 14* after influenza virus infection. Mice (eight per time point) were anesthetized with 0.3 ml FFM (0.079 mg/ml fentanyl citrate, 2.5 mg/ml fluanisone, and 1.25 mg/ml midazolam in H_2O; of this mixture 7.0 ml/kg intraperitoneally) and killed by bleeding out the vena cava inferior. Lungs were harvested and homogenized at 4°C in four volumes of sterile saline with a tissue homogenizer (Biospec Products, Bartlesville, OK). Hundred microliters of lung homogenates were treated with 1 ml of TRIzol reagent to extract RNA. RNA was resuspended in 10 μl of diethyl pyrocarbonate-treated water. cDNA synthesis was performed using 1 μl of the RNA suspension and a random hexamer cDNA synthesis kit (Applera, Foster City, CA). Two microliters out of 20 μl of cDNA suspension were used for amplification in real-time quantitative PCR reaction (Lightcycler Sequence Detector System; Roche, Mannheim, Germany). A standard curve was made using 10-fold dilutions of cDNA obtained from influenza virus-infected lung material. PAFR mRNA expression levels were normalized for the amount of TATA-box binding protein (TBP) mRNA present in each sample (1). The following primers were used: 5′-CTGGACCCTAGCAGAGTTGG-3′ (forward) and 5′-GCTACTGCGCATGCTGTAAA-3′ (reverse) for PAFR, 5′-CAGGAGCCAAGAGTGAAGAAC-3′ (forward) and 5′-GGAAATAATTCTGGCTCATAGCTACT-3′ (reverse) for TBP.

Determination of viral load in the lungs. Viral load was determined on *days 8* and *14* after viral infection and 48 h after pneumococcal infection (i.e., 16 days after viral infection) using real-time quantitative PCR as described (30, 31, 32). Five microliters out of 25 μl of cDNA suspension were used for amplification in a quantitative real-time PCR reaction (ABI PRISM 7700 Sequence Detector System). The viral load present in each sample was calculated with a standard curve of particle-counted influenza virus (virus particles were counted by electron microscopy), included in every assay. The following primers were used: 5′-GGACTGCAGCTGAGACGCT-3′ (forward); 5′-CATCCTGTTGTATATGAGGCCCAT-3′ (reverse) and 5′-CTCAGTTATTCTGCTGGTGCACTTGCC-3′ (5′-FAM-labeled probe).

Determination of bacterial outgrowth. Serial 10-fold dilutions of the lung homogenates in sterile saline and 10-μl volumes were plated out onto blood-agar plates. Plates were incubated at 37°C at 5% CO_2, and CFUs were counted after 16 h.

Histopathological analysis. Lungs for histological examination were harvested 48 h after pneumococcal infection, fixed in 10% formalin, and embedded in paraffin. Sections (4 μm) were stained with hematoxylin and eosin (H/E) and analyzed by a pathologist who was blinded for the groups.

Bronchoalveolar lavage. The trachea was exposed through a midline incision and cannulated with a sterile 22-gauge Abbocath-T catheter (Abbott, Sligo, Ireland). Bronchoalveolar lavage (BAL) was performed by instillation of two 0.5-ml aliquots of sterile saline into the right lung. The retrieved BAL fluid (BALF, ~0.8 ml) was spun at 260 *g* for 10 min at 4°C, and the pellet was resuspended in 0.5 ml of sterile PBS. Total cell numbers were counted using a Z2 Coulter Particle Count and Size Analyzer (Beckman-Coulter, Miami, FL). Differential cell counts were done on cytospin preparations stained with modified Giemsa stain (Diff-Quick, Baxter, UK).

Cytokine and chemokine measurements. Lung homogenates were lysed with an equal volume of lysis buffer [300 mM NaCl, 30 mM Tris, 2 mM $MgCl_2$, 2 mM $CaCl_2$, 1% (vol/vol) Triton X-100, 20 ng/ml pepstatin A, 20 ng/ml leupeptin, and 20 ng/ml aprotinin, pH 7.4] and incubated for 30 min on ice, followed by centrifugation at 680 *g* for 10 min. Supernatants were stored at −80°C until further use. Cytokines and chemokines in total lung lysates were measured by enzyme-linked immunosorbent assay according to the manufacturer's protocol. Reagents for interleukin (IL)-6, IL-10, cytokine-induced neutrophil chemoattractant (KC), and tumor necrosis factor (TNF)-α measurements were obtained from R&D systems (Abingdon, UK); interferon-γ reagents were obtained from Pharmingen (San Diego, CA).

Statistical analysis. All data are expressed as means ± SE, unless stated otherwise. Differences between groups were analyzed by Mann-Whitney *U*-test. Survival was analyzed with Kaplan-Meier using a log-rank test; $P < 0.05$ was considered to represent a statistically significant difference.

RESULTS

PAFR expression in the lungs after influenza virus infection in mice. PAFR expression in the lungs was determined by real-time PCR on *day 8* and *day 14* after influenza virus infection. A 10-fold increase in PAFR mRNA was observed on *day 8* after viral infection ($P = 0.0095$ vs. control mice, Fig. 1).

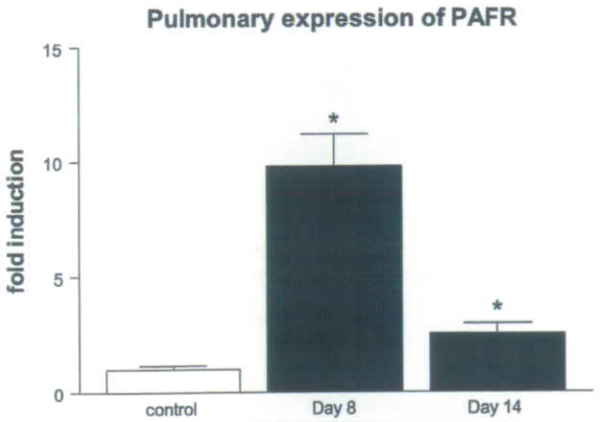

Fig. 1. Pulmonary expression of platelet-activating factor receptor (PAFR) after influenza virus infection. PAFR mRNA was measured by real-time quantitative PCR (8 mice per time point), except control group (4 mice). Expression levels were normalized for TATA-box binding protein mRNA expression levels. Data are expressed as fold induction over control (± SE). *$P < 0.05$ vs. control mice.

Although the expression of the PAFR declined thereafter, a 2.5-fold increase could still be observed on *day 14* after viral infection ($P = 0.0162$ vs. control mice). These data indicate that influenza virus induces the expression of PAFR in vivo.

Primary influenza virus infection. Viral load in the lungs was measured on *day 8* and *day 14* after infection to determine the role of the PAFR during primary influenza A infection. Viral load was similar in PAFR$^{-/-}$ and wild-type mice on *day 8* after infection (Fig. 2). On *day 14* after infection, both wild-type and PAFR$^{-/-}$ mice had cleared the virus completely. These data indicate that PAFR deficiency does not hamper the clearance of influenza A in vivo.

Prolonged survival during secondary pneumococcal infection in PAFR$^{-/-}$ mice. To investigate the role of the PAFR during secondary bacterial pneumonia we inoculated mice with *S. pneumoniae* on *day 14* after influenza infection. Lethality was monitored in PAFR$^{-/-}$ and wild-type mice (11 mice per group) during secondary pneumococcal pneumonia at least twice daily (Fig. 3). Influenza-recovered PAFR$^{-/-}$ mice displayed a prolonged survival after pneumococcal infection ($P = 0.014$ vs. wild-type mice).

Bacterial outgrowth. To obtain insight into the role of the PAFR in the outgrowth of pneumococci in lungs previously exposed to influenza A and in the dissemination of bacteria, lungs and blood were cultured 48 h after infection with *S. pneumoniae*. The number of *S. pneumoniae* CFU was threefold lower in PAFR$^{-/-}$ than in wild-type mice ($P = 0.05$, Fig. 4). Moreover, the PAFR played a role in the dissemination of *S. pneumoniae* into the circulation: only 57% of PAFR$^{-/-}$ mice had positive blood cultures vs. 100% of wild type, and the number of *S. pneumoniae* CFU in blood of PAFR$^{-/-}$ mice was lower than in wild-type mice ($P = 0.05$, Fig. 4).

Pulmonary cytokine and chemokine concentrations. Cytokines and chemokines play an important role in host defense against bacterial pneumonia (26). Therefore, to determine the effect of the PAFR on the induction of these mediators, the concentrations of TNF-α, IL-6, IL-10, and KC were measured in lung homogenates (Fig. 5). Lung levels of TNF-α, IL-6, and IL-10 were similar in wild-type mice and PAFR$^{-/-}$ mice on *day 14* after influenza infection (Fig. 5), whereas KC production was slightly reduced in PAFR$^{-/-}$ mice ($P = 0.0317$ vs. wild-type mice). *S. pneumoniae* infection on *day 14* after influenza resulted in enhanced production of TNF-α, IL-6, IL-10, and KC (Fig. 5). On *day 16*, i.e., 48 h after *S. pneumoniae* infection, IL-10 and KC levels were significantly lower in PAFR$^{-/-}$ mice than in wild-type mice ($P < 0.05$). Lung levels of TNF-α and IL-6 tended to be lower in PAFR$^{-/-}$ mice, but the difference with wild-type mice was not statistically significant ($P = 0.16$ and $P = 0.09$ respectively).

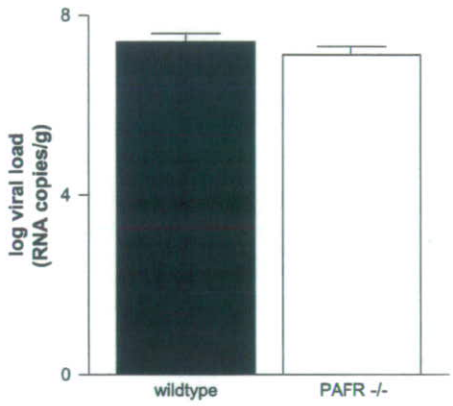

Fig. 2. Viral load in the lungs on *day 8* after influenza infection. Viral load is expressed as RNA copies per gram lung tissue (means ± SE) as determined by real-time PCR (5–8 mice per group). Both wild-type mice (filled bar) and PAFR$^{-/-}$ mice (open bar) had cleared the virus on *day 14* after infection (data not shown).

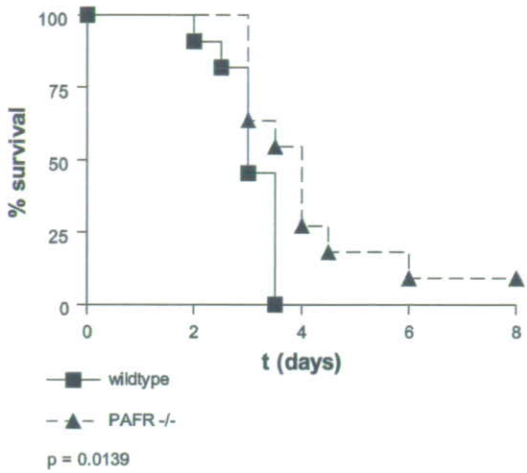

Fig. 3. Prolonged survival in PAFR$^{-/-}$ mice after secondary bacterial pneumonia. Survival after pneumococcal infection in influenza-recovered PAFR$^{-/-}$ mice (▲) vs. wild-type mice (■). All mice (11 mice per group) received 10^4 colony-forming units (CFU) of *Streptococcus pneumoniae* on *day 14* after viral infection and were monitored at least twice a day after pneumococcal infection.

Cell influx in BALF. Neutrophils play a pivotal role in host defense against bacterial pneumonia (26). Because inhibition of PAFR function has been shown to reduce leukocyte influx into the lungs in response to intrapulmonary delivery of killed pneumococci (16), we assessed the number of leukocytes recruited to the alveoli. Although total cell counts tended to be lower in BALF obtained from PAFR$^{-/-}$ mice than in BALF from wild-type mice, this difference was not statistically significant. The relative number of neutrophils was trendwise lower in PAFR$^{-/-}$ mice ($P = 0.09$ vs. wild-type mice, Table 1), whereas the relative number of macrophages was trendwise higher in PAFR$^{-/-}$ mice ($P = 0.09$ vs. wild-type mice, Table 1).

Histopathology. Forty-eight hours after pneumococcal infection, lungs were harvested to prepare H/E-stained lung slides for histopathological examination. Mice recovered from influenza infection with secondary pneumococcal pneumonia showed severe interstitial inflammation, bronchiolitis, endothelialitis, and pleuritis in the lungs. No significant differences were observed between wild-type mice and PAFR$^{-/-}$ mice (Fig. 6).

DISCUSSION

Secondary pneumococcal pneumonia is a serious complication of influenza A infection. The increased susceptibility to secondary bacterial infections during and shortly after influenza is, at least in part, due to enhanced colonization and interaction of the respiratory epithelium with *S. pneumoniae*

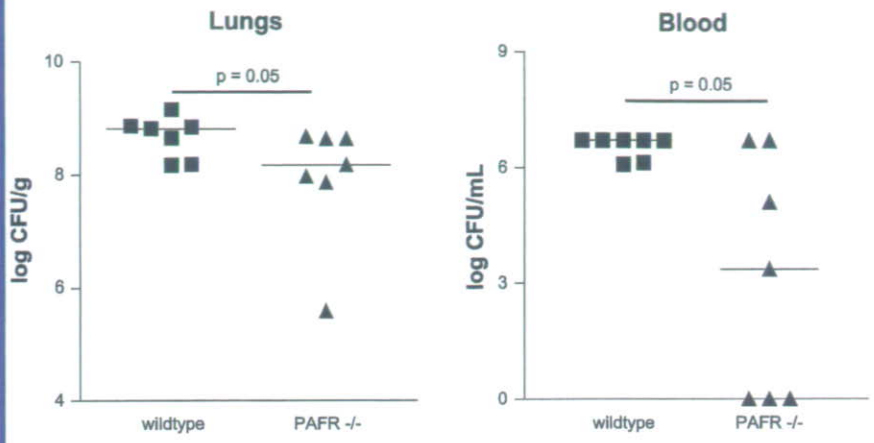

Fig. 4. Reduced bacterial outgrowth in the lungs and blood of PAFR$^{-/-}$ mice. Bacterial outgrowth in the lungs (*left*) and blood (*right*) after pneumococcal infection in wild-type mice (■) and PAFR$^{-/-}$ mice (▲). All mice (7 mice per group) received 10^4 CFU *S. pneumoniae* on *day 14* after viral infection and were killed 48 h later. Horizontal lines represent medians for each group. Note that 3 PAFR$^{-/-}$ mice had no bacteria in their blood 48 h after infection.

(14, 16, 28). Because the PAFR has been described to be upregulated during viral infections (10) and since the PAFR facilitates invasion of the pneumococcus through epithelial cells through binding of phosphorylcholine in the cell wall of *S. pneumoniae* (3), it has been suggested that the PAFR may play a critical role during postinfluenza pneumococcal pneumonia (11). In the present study we show that influenza virus infection in mice results in increased PAFR expression in the lungs on *day 8* and *day 14* after infection. In addition, targeted deletion of the PAFR improves host defense against *S. pneumoniae* in a mouse model for secondary bacterial pneumonia, as reflected by prolonged survival and reduced bacterial loads in the lungs and the circulation.

Our data are contradictory to a previous study by McCullers and Rehg (11), who showed that influenza-infected mice treated with CV-6209, a PAFR antagonist, displayed enhanced outgrowth of pneumococci (72 h after infection). Although several differences between our investigation and that of McCullers and Rehg (11) can be pointed out, including differences in the *S. pneumoniae* strains used (ATCC 6303, *serotype 3* vs. D39, *serotype 2*, respectively) and differences in the interval between influenza and secondary pneumococcal infection (14 vs. 7 days, respectively), the data reported by McCullers and Rehg are difficult to explain in the context of current knowledge on the role of the PAFR in pneumococcal infection. Indeed, these authors observed a reduced rather than an increased host defense after administration of a PAFR antagonist during primary pneumococcal pneumonia (10), which contrasts with three earlier investigations addressing this topic (2, 3, 20). Our own laboratory found that PAFR$^{-/-}$ mice display enhanced survival and reduced bacterial outgrowth after primary pneumococcal pneumonia (20). Similarly, intratracheal PAFR antagonist treatment during pneumococcal infection in rabbits resulted in reduced bacterial loads in the lung (3). Conceivably, the specific properties of the PAFR antagonist used by McCullers and Rehg (11) may have played a role. Hence, our current data seem to indicate that the pneumococcus uses the PAFR to invade the respiratory epithelium of the

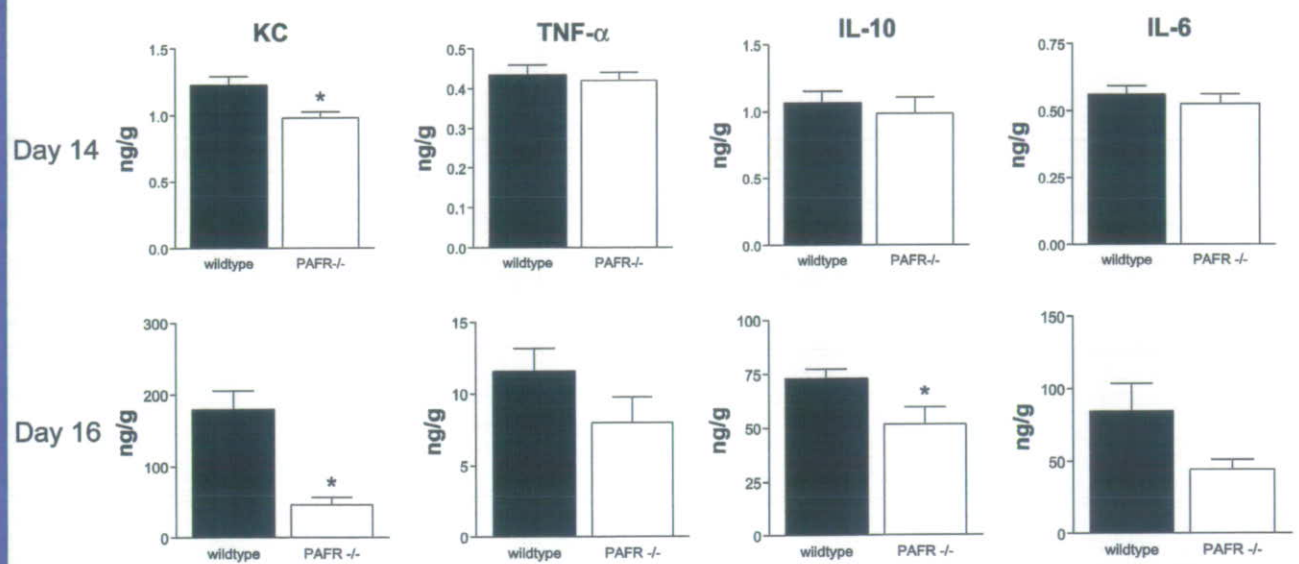

Fig. 5. Cytokine levels in the lungs on *day 14* (influenza) and *day 16* (influenza + *S. pneumoniae*): KC, TNF-α, IL-10, and IL-6 in wild-type (filled bars) and PAFR$^{-/-}$ mice (open bars) at 48 h after secondary bacterial pneumonia. Data are expressed in ng/g lung tissue (means ± SE, 5–7 mice per group). Please note that the *x*-axis scales differ between the *top* and *bottom* panels (mediator levels before bacterial pneumonia were much lower). *$P < 0.05$ vs. wild-type mice

Table 1. *Leukocytes in BALF 48 h after secondary bacterial pneumonia*

Cells, $\times 10^3$	Wild-type Mice	PAFR$^{-/-}$ Mice
Total cell count	1,398±411	782±335
Neutrophils (%)	1,046±325 (67.2%)	458±184 (52.5%)
Macrophages (%)	336±98 (31.5%)	321±164 (46.8%)
Lymphocytes (%)	16.2±9.8 (1.3%)	2.9±1.5 (0.7%)

Leukocyte counts (6 mice per group) are expressed as absolute numbers ($\times 10^3$) and percentages of total cell count. All data are means ± SE. No statistically significant differences were found between wild-type and PAFR$^{-/-}$ mice 48 h after secondary pneumococcal pneumonia. PAFR, platelet-activating factor receptor; BALF, bronchoalveolar lavage fluid.

host previously exposed to influenza A. As such, the involvement of the PAFR in the pathogenesis of primary and postinfluenza pneumococcal pneumonia seems quite similar (20).

Of note, in our study, an interval of 14 days between viral and bacterial infection was chosen to exclude a direct interaction between influenza virus and *S. pneumoniae*. Previous studies by our group have indicated that influenza virus is completely cleared from the lungs of wild-type mice on *day 14* after infection (32), which was confirmed here. The present study establishes that clearance of influenza A is not altered in PAFR$^{-/-}$ mice: viral loads were similar in PAFR$^{-/-}$ and wild-type mice 8 days after infection and both strains had cleared the virus completely on *day 14*, the day on which pneumococcal pneumonia was induced. These findings not only revealed that the PAFR does not contribute to host defense against influenza A to a significant extent but also allowed us to use PAFR$^{-/-}$ mice to study the role of the PAFR during postinfluenza pneumococcal pneumonia.

The improved outcome observed in PAFR$^{-/-}$ mice could also be explained by the release of protective mediators after pneumococcal infection. Pulmonary levels of KC were significantly lower in PAFR$^{-/-}$ mice than in wild-type mice on *day 14* after primary influenza infection and after secondary bacterial challenge; TNF-α and IL-6 levels were only trendwise lower. Because secondary pneumococcal infection resulted in a 100-fold increase in KC levels, it seems unlikely that the reduced KC levels on *day 14* after primary influenza infection contributed to the final outcome of secondary bacterial pneumonia. The reduced KC levels after secondary bacterial infection may at least in part account for the reduced neutrophil numbers in BALF, which is line with previous studies that indicate that pulmonary KC levels correlate with neutrophil influx during *S. pneumoniae* and *P. aeruginosa* infection in mice (4, 19, 27, 29). Alternatively, and not mutually exclusive, the tendency toward a reduced inflammatory response in lungs of PAFR$^{-/-}$ mice, which was also observed after primary pneumococcal pneumonia (20), could be the consequence of a lower bacterial load (providing a less potent proinflammatory stimulus) in the lungs (4).

We have previously shown that mice recovered from influenza produce high amounts of cytokines and excessive lung inflammation after induction of secondary pneumococcal pneumonia when compared with mice suffering from primary bacterial infection (30).

Because PAFR activation results in a proinflammatory stimulus, one could argue that the enhanced inflammatory reaction is partially due to PAFR expression in mice exposed to influenza. Indeed, the PAFR appears to be particularly important for the induction of pulmonary inflammation. Pretreatment with PAFR antagonists strongly diminished pulmonary vascular leakage and edema after systemic or intrapulmonary injection of lipopolysaccharide (13, 21, 23). Studies by Nagase et al. (15) revealed a critical role for the PAFR during acid aspiration in mice. Our current data argue against an important role for the PAFR in the exaggerated lung inflammation in mice with postinfluenza pneumonia, if one considers that PAFR$^{-/-}$ mice only showed a tendency toward reduced levels of proinflammatory cytokines (IL-6, TNF-α) and trendwise reduced neutrophils in their lungs. Besides, pulmonary levels of the anti-inflammatory cytokine IL-10 were modestly reduced as well. Of note, in theory, the proinflammatory properties of PAF and PAF-like lipids, such as phosphorylcholine, would make these phospholipid mediators potential protective mediators during pneumonia (2). Indeed, PAFR$^{-/-}$ mice displayed enhanced bacterial outgrowth in a mouse model for *Klebsiella pneumoniae*, a bacterium that does not express phosphorylcholine (25). This study supports the importance of phosphorylcholine binding by the PAFR during primary and secondary pneumococcal pneumonia.

S. pneumoniae is the main causative pathogen in postinfluenza pneumonia. In vitro studies have established that this bacterium can invade tissues by an interaction between phosphorylcholine present in its cell wall and the PAFR expressed by epithelial cells. We demonstrate here that the pneumococcus uses the PAFR to accomplish severe pneumonia in mice previously exposed to influenza. The fact that lethality also occurred in PAFR$^{-/-}$ mice indicates that the PAFR is not

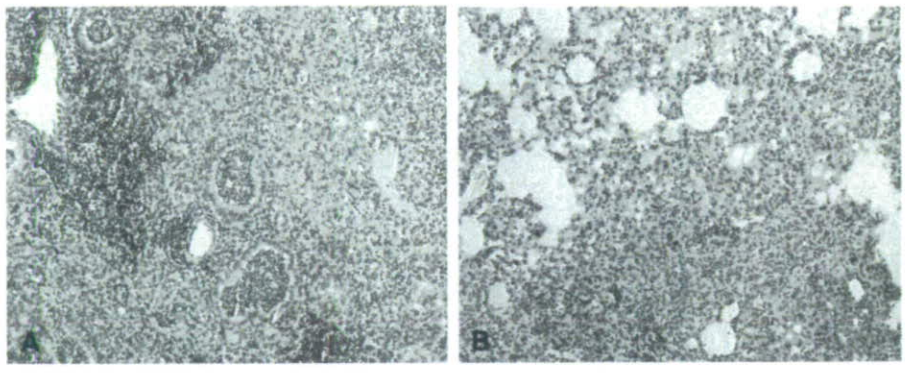

Fig. 6. Histopathological analysis. Inflammatory response upon pneumococcal infection in wild-type mice (*A*) and PAFR$^{-/-}$ mice (*B*) after recovery from influenza virus. Mice received 10^4 CFU *S. pneumoniae* on *day 14* after viral infection and were killed 48 h later. Lung slides were stained by hematoxylin and eosin (original magnification ×33). Representative slides of 6 mice per group are shown.

mandatory for tissue invasion but, rather, that this receptor increased the potential virulence of *S. pneumoniae* in the respiratory tract. As such, the role of the PAFR in primary (20) and secondary (this study) pneumococcal pneumonia does not seem to differ significantly.

ACKNOWLEDGMENTS

We thank Joost Daalhuisen and Ingvild Kop for technical assistance during the animal experiments, Teus van den Ham for assistance during the preparation and titration of the viral stocks, and Jan Aten for the development of the quantitative PCR for TBP mRNA.

Present address of S. Ishii: Dept. of Biochemistry and Molecular Biology, Faculty of Medicine, The University of Tokyo, Tokyo, Japan.

REFERENCES

1. **Almeida A, Paul Thiery J, Magdelenat H, and Radvanyi F.** Gene expression analysis by real-time reverse transcription polymerase chain reaction: influence of tissue handling. *Anal Biochem* 328: 101–108, 2004.
2. **Cabellos C, MacIntyre DE, Forrest M, Burroughs M, Prasad S, and Tuomanen E.** Differing roles for platelet-activating factor during inflammation of the lung and subarachnoid space. The special case of *Streptococcus pneumoniae*. *J Clin Invest* 90: 612–618, 1992.
3. **Cundell DR, Gerard NP, Gerard C, Idanpaan-Heikkila I, and Tuomanen EI.** Streptococcus pneumoniae anchor to activated human cells by the receptor for platelet-activating factor. *Nature* 377: 435–438, 1995.
4. **Dallaire F, Ouellet N, Bergeron Y, Turmel V, Gauthier MC, Simard M, and Bergeron MG.** Microbiological and inflammatory factors associated with the development of pneumococcal pneumonia. *J Infect Dis* 184: 292–300, 2001.
5. **Fischer W.** Phosphocholine of pneumococcal teichoic acids: role in bacterial physiology and pneumococcal infection. *Res Microbiol* 151: 421–427, 2000.
6. **Hirano T, Kurono Y, Ichimiya I, Suzuki M, and Mogi G.** Effects of influenza A virus on lectin-binding patterns in murine nasopharyngeal mucosa and on bacterial colonization. *Otolaryngol Head Neck Surg* 121: 616–621, 1999.
7. **Ishii S, Kuwaki T, Nagase T, Maki K, Tashiro F, Sunaga S, Cao WH, Kume K, Fukuchi Y, Ikuta K, Miyazaki J, Kumada M, and Shimizu T.** Impaired anaphylactic responses with intact sensitivity to endotoxin in mice lacking a platelet-activating factor receptor. *J Exp Med* 187: 1779–1788, 1998.
8. **Ishii S, Matsuda Y, Nakamura M, Waga I, Kume K, Izumi T, and Shimizu T.** A murine platelet-activating factor receptor gene: cloning, chromosomal localization and up-regulation of expression by lipopolysaccharide in peritoneal resident macrophages. *Biochem J* 314: 671–678, 1996.
9. **Ishizuka S, Yamaya M, Suzuki T, Nakayama K, Kamanaka M, Ida S, Sekizawa K, and Sasaki H.** Acid exposure stimulates the adherence of *Streptococcus pneumoniae* to cultured human airway epithelial cells: effects on platelet-activating factor receptor expression. *Am J Respir Cell Mol Biol* 24: 459–468, 2001.
10. **Ishizuka S, Yamaya M, Suzuki T, Takahashi H, Ida S, Sasaki T, Inoue D, Sekizawa K, Nishimura H, and Sasaki H.** Effects of rhinovirus infection on the adherence of *Streptococcus pneumoniae* to cultured human airway epithelial cells. *J Infect Dis* 188: 1928–1939, 2003.
11. **McCullers JA and Rehg JE.** Lethal synergism between influenza virus and *Streptococcus pneumoniae*: characterization of a mouse model and the role of platelet-activating factor receptor. *J Infect Dis* 186: 341–350, 2002.
12. **McCullers JA and Tuomanen EI.** Molecular pathogenesis of pneumococcal pneumonia. *Front Biosci* 6: D877–D889, 2001.
13. **Miotla JM, Jeffery PK, and Hellewell PG.** Platelet-activating factor plays a pivotal role in the induction of experimental lung injury. *Am J Respir Cell Mol Biol* 18: 197–204, 1998.
14. **Murphy BR and Webster RG.** Orthomyxoviruses. In: *Fields Virology* (3rd ed.), Philadelphia, PA: Lippincott-Raven, 1996, p. 1407.
15. **Nagase T, Ishii S, Kume K, Uozumi N, Izumi T, Ouchi Y, and Shimizu T.** Platelet-activating factor mediates acid-induced lung injury in genetically engineered mice. *J Clin Invest* 104: 1071–1076, 1999.
16. **O'Brien KL, Walters MI, Sellman J, Quinlisk P, Regnery H, Schwartz B, and Dowell SF.** Severe pneumococcal pneumonia in previously healthy children: the role of preceding influenza infection. *Clin Infect Dis* 30: 784–789, 2000.
17. **Plotkowski MC, Puchelle E, Beck G, Jacquot J, and Hannoun C.** Adherence of type I *Streptococcus pneumoniae* to tracheal epithelium of mice infected with influenza A/PR8 virus. *Am Rev Respir Dis* 134: 1040–1044, 1986.
18. **Reed LJ and Muench H.** A simple method of estimating fifty percent endpoints. *Am J Hyg* 27: s493–s497, 1938.
19. **Remick DG, Green LB, Newcomb DE, Garg SJ, Bolgos GL, and Call DR.** CXC chemokine redundancy ensures local neutrophil recruitment during acute inflammation. *Am J Pathol* 159: 1149–1157, 2001.
20. **Rijneveld AW, Weijer S, Florquin S, Speelman P, Shimizu T, Ishii S, and van der Poll T.** Improved host defense against pneumococcal pneumonia in platelet-activating factor receptor-deficient mice. *J Infect Dis* 189: 711–716, 2004.
21. **Rylander R, Beijer L, Lantz RC, Burrell R, and Sedivy P.** Modulation of pulmonary inflammation after endotoxin inhalation with a platelet-activating factor antagonist (48740 RP). *Int Arch Allergy Appl Immunol* 86: 303–307, 1988.
22. **Shirasaki H, Nishikawa M, Adcock IM, Mak JC, Sakamoto T, Shimizu T, and Barnes PJ.** Expression of platelet-activating factor receptor mRNA in human and guinea pig lung. *Am J Respir Cell Mol Biol* 10: 533–537, 1994.
23. **Siebeck M, Weipert J, Keser C, Kohl J, Spannagl M, Machleidt W, and Schweiberer L.** A triazolodiazepine platelet activating factor receptor antagonist (WEB 2086) reduces pulmonary dysfunction during endotoxin shock in swine. *J Trauma* 31: 942–949, 1991.
24. **Simon HU, Tsao PW, Siminovitch KA, Mills GB, and Blaser K.** Functional platelet-activating factor receptors are expressed by monocytes and granulocytes but not by resting or activated T and B lymphocytes from normal individuals or patients with asthma. *J Immunol* 153: 364–377, 1994.
25. **Soares AC, Pinho VS, Souza DG, Shimizu T, Ishii S, Nicoli JR, and Teixeira MM.** Role of the platelet-activating factor (PAF) receptor during pulmonary infection with gram negative bacteria. *Br J Pharmacol* 137: 621–628, 2002.
26. **Strieter RM, Belperio JA, and Keane MP.** Cytokines in innate host defense in the lung. *J Clin Invest* 109: 699–705, 2002.
27. **Tateda K, Moore TA, Newstead MW, Tsai WC, Zeng X, Deng JC, Chen G, Reddy R, Yamaguchi K, and Standiford TJ.** Chemokine-dependent neutrophil recruitment in a murine model of *Legionella pneumonia*: potential role of neutrophils as immunoregulatory cells. *Infect Immun* 69: 2017–2024, 2001.
28. **Treanor JJ.** Orthomyxoviridae: influenza virus. In: *Principles and Practice of Infectious Diseases* (5th ed.), New York: Churchill Livingston, 2000, p. 1834–1835.
29. **Tsai WC, Strieter RM, Mehrad B, Newstead MW, Zeng X, and Standiford TJ.** CXC chemokine receptor CXCR2 is essential for protective innate host response in murine *Pseudomonas aeruginosa* pneumonia. *Infect Immun* 68: 4289–4296, 2000.
30. **Van Elden LJR, Nijhuis M, Schipper P, Schuurman R, and van Loon AM.** Simultaneous detection of influenza virus A and B using real-time quantitative PCR. *J Clin Microbiol* 39: 196–200, 2001.
31. **Van der Sluijs KF, Van Elden L, Nijhuis M, Schuurman R, Florquin S, Jansen HM, Lutter R, and Van der Poll T.** Toll-like receptor 4 is not involved in host defense against respiratory tract infection with Sendai virus. *Immunol Lett* 89: 201–206, 2003.
32. **Van der Sluijs KF, Van Elden LJR, Nijhuis M, Schuurman R, Pater JM, Florquin S, Goldman M, Jansen HM, Lutter R, and Van der Poll T.** IL-10 is an important mediator of the enhanced susceptibility to pneumococcal pneumonia after influenza infection. *J Immunol* 172: 7603–7609, 2004.

American Journal of Pathology, Vol. 168, No. 5, May 2006

DOI: 10.2353/ajpath.2006.050634

Cardiovascular, Pulmonary and Renal Pathology

Attenuation of Folic Acid-Induced Renal Inflammatory Injury in Platelet-Activating Factor Receptor-Deficient Mice

Kent Doi,* Koji Okamoto,* Kousuke Negishi,* Yoshifumi Suzuki,* Akihide Nakao,* Toshiro Fujita,* Akiko Toda,*† Takehiko Yokomizo,† Yoshihiro Kita,† Yasuyuki Kihara,† Satoshi Ishii,† Takao Shimizu,†‡ and Eisei Noiri*‡

From the Departments of Nephrology and Endocrinology, and Biochemistry and Molecular Biology,† and the Center for NanoBio Integration,‡ University of Tokyo, Tokyo, Japan*

Platelet-activating factor (PAF), a potent lipid mediator with various biological activities, plays an important role in inflammation by recruiting leukocytes. In this study we used platelet-activating factor receptor (PAFR)-deficient mice to elucidate the role of PAF in inflammatory renal injury induced by folic acid administration. PAFR-deficient mice showed significant amelioration of renal dysfunction and pathological findings such as acute tubular damage with neutrophil infiltration, lipid peroxidation observed with antibody to 4-hydroxy-2-hexenal (day 2), and interstitial fibrosis with macrophage infiltration associated with expression of monocyte chemoattractant protein-1 and tumor necrosis factor-α in the kidney (day 14). Acute tubular damage was attenuated by neutrophil depletion using a monoclonal antibody (RB6-8C5), demonstrating the contribution of neutrophils to acute phase injury. Macrophage infiltration was also decreased when treatment with a PAF antagonist (WEB2086) was started after acute phase. *In vitro* chemotaxis assay using a Boyden chamber demonstrated that PAF exhibits a strong chemotactic activity for macrophages. These results indicate that PAF is involved in pathogenesis of folic acid-induced renal injury by activating neutrophils in acute phase and macrophages in chronic interstitial fibrosis. Inhibiting the PAF pathway might be therapeutic to kidney injury from inflammatory cells. *(Am J Pathol 2006, 168:1413–1424; DOI: 10.2353/ajpath.2006.050634)*

Inflammation is an important component of renal injury, in both acute renal failure[1,2] and chronic renal damage that accompanies interstitial fibrosis.[3,4] The infiltrating inflammatory cells contribute to renal damage through generation of reactive oxygen species (ROS), further recruitment of leukocytes, and production of proinflammatory and profibrotic cytokines. Therefore, the mechanism of directing circulating leukocytes to the kidney and maintaining them there is a potential target for therapeutic intervention for kidney diseases.

Platelet-activating factor (PAF; 1-*O*-alkyl-2-acethl-*sn*-glycero-3-phosphocholine) is a potent proinflammatory phospholipid mediator with various biological effects such as activating platelets, neutrophils, eosinophils, and macrophages. PAF binds to a G-protein-coupled seven transmembrane receptor, PAF receptor (PAFR); PAF plays an important role in the pathophysiology of inflammatory conditions.[5,6] Synthesis of PAF has been demonstrated not only in blood cells but in the kidney under physiological conditions,[7] ischemia reperfusion injury,[8] and clipped kidney.[9] Treatment with several PAF antagonists has been reported in acute renal failure[10] and chronic renal failure animal models.[11,12] However, problems exist regarding the lack of specificity of PAF antagonists.[13–16] Therefore, we have developed genetically engineered PAFR-deficient (PAFR-KO) mice to confirm the role of PAF *in vivo*.[17] The resultant PAFR-KO mice exhibit attenuated symptoms in several animal models such as chemical lung injury,[18] bronchial asthma,[19] and sponge-induced subcutaneous granuloma formation.[20] It

Supported in part by grants from the Cell Science Research Foundation, Osaka, Japan (to E.N.); the Araki Memorial Research Foundation for Medicine and Biochemistry, Tokyo, Japan (to E.N.); Takeda Medical Science, Osaka, Japan (to E.N.); and the Health and Labour Science research grants for Research on Human Genome, Tissue Engineering, and Food Biotechnology from the Ministry of Health, Labour, and Welfare of Japan (to E.N.).

K.D. and K.O. contributed equally to this work.

Accepted for publication January 10, 2006.

Address reprint requests to Dr. Eisei Noiri, M.D., Ph.D., Department of Nephrology and Endocrinology, University of Tokyo, 7-3-1 Hongo, Bunkyo, Tokyo 113-8655, Japan. E-mail: noiri-tky@umin.ac.jp.

has been demonstrated that infiltrating inflammatory cells play important roles in these animal models.

The folic acid (FA)-induced renal injury model has been applied recently for evaluation of epithelial regeneration and interstitial fibrosis.[21–24] Intraperitoneal administration of FA with sodium bicarbonate induced renal injury that showed acute tubular necrosis with transient elevations of blood urea nitrogen (BUN) and serum creatinine (Cr) followed by development of interstitial fibrosis with macrophage infiltration.[21,25] Tubular obstructions by FA crystals and direct toxic effect of FA to tubular epithelial cells presumably cause renal damage,[26] but the precise mechanism of injury remains unclear. Inflammatory cell infiltrations were remarkable in injured kidneys of this model.

Here we examined the role of PAF in inflammatory renal injury induced by FA administration. Using PAFR-KO mice, we show attenuation of renal injury not only in cases of acute tubular damage but also in cases of development of chronic interstitial fibrosis *in vivo*. In addition, we evaluated the effects of neutrophil depletion and PAF antagonist treatment after the acute phase to confirm the contribution of leukocytes to FA-induced renal injury. We also demonstrate the role of PAF as a strong chemoattractant for macrophages *in vitro*, indicating that PAF blockade can prevent progression of inflammatory damage in kidney.

Materials and Methods

Reagents

Folic acid was obtained from Sigma Chemical Co. (St. Louis, MO) and WEB2086 was a generous gift from Boehringer (Ingelheim, Germany). We used a mouse antibody to 4-hydroxy-2-hexenal (HHE)-modified protein, in which the aldehyde HHE is derived from the oxidative process of polyunsaturated fatty acid, obtained from NOF Corp. (Tokyo, Japan) and a mouse anti-smooth muscle α actin (α-SMA) monoclonal antibody (1A4) (DakoCytomation Co. Ltd., Glostrup, Denmark) for immunohistochemical and Western blot analyses. We used a rat anti-mouse neutrophil antibody (Caltag Laboratories, Burlingame, CA), a rat anti-mouse F4/80 macrophage antigen antibody (MCA497R) (Serotec, Raleigh, NC), and a goat anti-mouse MCP-1/JE antibody (Santa Cruz Biotechnology Inc., Santa Cruz, CA) for immunohistochemical analyses. The monoclonal antibody RB6-8C5 was used for neutrophil depletion. It is a rat IgG2b that selectively binds to and depletes mature neutrophils but not lymphocytes or macrophages.[27–31] The hybridoma that secretes this antibody was a gift from Dr. R. Coffman (DNAX Research Inc., Palo Alto, CA); RB6-8C5 from hybridoma culture supernatants was purified through ammonium sulfate precipitation. All other chemicals were purchased from Wako Pure Chemical Industries Ltd. (Osaka, Japan) unless otherwise specified.

Animal Model

We established PAFR-KO mice as described previously.[17] The PAFR-KO mice and the corresponding wild-type (PAFR-WT) mice were backcrossed for 10 generations onto a C57BL/6N genetic background. Mice were allowed food and water *ad libitum*, and experiments were conducted in accordance with the Guide for the Care and Use of Laboratory Animals [Department of Health, Education and Welfare Publication No. (NIH) 86-23, Revised 1985, Office of Science and Health Reports, DRR/NIH, Bethesda, MD]. Male and female mice used for this study were 9 to 11 weeks of age, weighing 18 to 25 g. Within each experimental group, the sex ratio, age, and weight of animals did not differ significantly. The animals were anesthetized with diethyl ether and administered FA by intraperitoneal injection at the dose of 250 mg/kg in vehicle (0.5 ml of 0.3 mmol/L $NaHCO_3$) or given vehicle alone. The dose of FA and $NaHCO_3$ was critical for induction of severe renal damage and was determined by preliminary studies. Blood was drawn from the tail vein of each animal, and the levels of BUN and Cr were measured 3 days before and at 2, 7, and 14 days after FA administration by the urease-indophenol method with Urea N B (Wako Pure Chemical Industries Ltd.) and the colorimetric method based on hydrogen peroxide measurement with Nescoat VLII CRE (Alfresa Pharma Corp., Osaka, Japan), respectively. Kidneys were removed 2 and 14 days after FA administration and fixed in 10% buffered formalin for staining with hematoxylin and eosin, Masson's trichrome, and immunochemical staining, except for mouse neutrophil detection for which methyl Carnoy's solution was used. Parts of kidneys were snap-frozen for immunohistochemical testing of MCP-1; they were otherwise used for Western blot analysis and real-time polymerase chain reaction (PCR) assay.

For neutrophil depletion experiments, PAFR-WT mice were treated with 50 μg of monoclonal antibody RB6-8C5. Injection of FA was performed the following day, and the animals were sacrificed 2 days after FA administration. Injection of 25 μg of monoclonal antibody RB6-8C5 was reported to cause significant neutrophil depletion from the subsequent day up to 3 days.[32–34] Blood collected at sacrifice was used for flow cytometry analyses to confirm neutrophil depletion. Mice that were untreated with RB6-8C5 served as control animals. To clarify the contribution of PAF for macrophage recruitment after initial damage, we intraperitoneally injected PAF antagonist (WEB2086) into PAFR-WT mice every day from day 2 to day 14 at the dose of 5 mg/kg and examined renal function (days 2, 7, and 14), macrophage infiltration, and interstitial fibrosis (day 14).

Flow Cytometry Analysis

Heparinized blood was incubated with anti-Gr-1 antibodies conjugated to fluorescein isothiocyanate (BD Pharmingen, San Diego, CA), and then Flowcount fluorospheres (Beckman Coulter Inc., Villepinte, France) were added. After red blood cell lysis with NH_4Cl buffer, cell suspen-

sion was run on a FACScan flow cytometer (Becton Dickinson Immunocytometry Systems, San Jose, CA), and the absolute count of Gr-1-positive cells was calculated using standardized Flowcount beads.

Morphological Evaluation of Kidneys

The area of the interstitial fibrosis in the cortex was evaluated with Masson's trichrome staining using a computer-aided evaluation program (AIS version 4.0; Fuji Photo Film Co. Ltd., Tokyo, Japan). Viewed at ×400 magnification, 10 randomly selected nonoverlapping fields from the cortical region were analyzed. The fibrotic areas stained in blue were depicted in digital images; then the percentage of the fibrotic area was calculated relative to the entire field area (percentage area). Glomeruli and large vessels were not included in the microscopic fields for image analysis. The degree of neutrophil and macrophage infiltration was measured as the average number of positive staining cells per field. The number of positively stained cells was determined in five randomly selected nonoverlapping fields at ×200 magnification in each section of the individual mouse renal cortex. Scores of respective kidneys as well as scores of each animal were averaged.

Western Blot Analysis

Western blot analyses were performed as described previously.[35] Briefly, harvested kidneys were homogenized on ice in a radioimmunoprecipitation assay buffer with protease inhibitors. The lysates were separated electrophoretically on a 10% polyacrylamide gel. After transferring proteins from the gel to a nitrocellulose membrane, Western blot analyses were performed using HHE or α-SMA antibody. After incubation with horseradish peroxidase-conjugated appropriate second antibody, chemiluminescent signal detection (ECL Plus; Amersham Biosciences Corp., Uppsala, Sweden) was performed using a cooled charge-coupled device camera system (LAS-1000; Fuji Photo Film Co. Ltd.). The membrane was incubated at 50°C for 30 minutes in a stripping buffer to remove all probes. Then it was reprobed with the antibody to α-tubulin (Santa Cruz Biotechnology Inc.). Densitometric analyses of bands compared with the density of α-tubulin were performed using National Institutes of Health Image software, version 1.62.

Immunohistochemical Analysis

Immunohistochemical staining of 2-μm paraffin sections was performed using indirect immunohistochemical techniques. Biotin-free immunohistochemical staining using horseradish peroxidase-conjugated polymer system was conducted according to the manufacturer's protocols (Histofine Mouse Stain kit and Histofine Simple Stain mouse MAX-PO (rat) kit; Nichirei Corp., Tokyo, Japan). The deparaffinized sections were preincubated with 0.3% hydrogen peroxide for 15 minutes and incubated with primary antibodies overnight at 4°C, followed by polymer-conjugated anti-mouse IgG. Protease K treatment was necessary for anti-F4/80 antibody; autoclaving in 10 mmol/L citrate-buffer (pH 6.0) was necessary for anti-HHE and anti-α-SMA antibody. For neutrophil staining, fixation with methyl Carnoy's solution was indispensable.[36] Diaminobenzidine tetrahydrochloride (Nichirei Corp.) was used for the substrate-chromogen reaction followed by counter staining with hematoxylin.

We used frozen sections of kidney to determine the immunohistochemistry of MCP-1, as described previously[37] but with modifications. With 8-μm cryostat sections fixed in acetone and goat anti-mouse MCP-1 antibody (Santa Cruz Biotechnology Inc.), a Vectastain Elite ABC kit (Vector Laboratories Inc., Burlingame, CA) and diaminobenzidine tetrahydrochloride were applied in accordance with the manufacturers' instructions. Sections were counterstained with methyl green (Vector Laboratories Inc.).

Real-Time PCR Assay for TNF-α and MCP-1 Expression

Harvested kidneys were homogenized with a homogenizer (Ultra-Turrax T8; IKA Labortechnik, Staufen, Germany) in Trizol total RNA isolation reagent (Invitrogen Corp., Carlsbad, CA). Total RNA was isolated by the acid guanidinium isothiocyanate-phenol-chloroform extraction method according to the manufacturer's protocols and treated with DNase I to remove potential contamination of DNA (DNA-free; Ambion Inc., Austin, TX). The mRNA was then reverse-transcribed to cDNA using MLV reverse transcriptase (RiverTra Ace; Toyobo Co. Ltd., Osaka, Japan) with random hexamers. Transcripts encoding tumor necrosis factor (TNF)-α and monocyte chemoattractant protein (MCP)-1 were measured using TaqMan real-time quantitative PCR with Prism 7000 sequence detection system (Applied Biosystems, Foster City, CA) using TaqMan universal PCR master mix (Applied Biosystems) according to the manufacturer's specifications. The TaqMan probes and primers for TNF-α (assay identification number Mm00443258_m1) and MCP-1 (assay identification number Mm00441242_m1) were assay-on-demand gene expression products (Applied Biosystems). The PCR reaction conditions were 95°C for 10 minutes, followed by 40 cycles of 95°C for 15 seconds and 60°C for 1 minute. To normalize for variance in loaded cDNA, 18S ribosomal RNA were amplified in a separate tube. Amplification data were analyzed using Applied Biosystems' Prism sequence detection software version 2.1 (Applied Biosystems). Standard curves were prepared for each gene and the 18S ribosomal RNA in each experiment to normalize the relative expression of the genes of interest to the 18S ribosomal RNA control.

Measurement of PAF Levels in Kidney

Harvested kidneys were frozen immediately with liquid nitrogen at days 2 and 14. The PAF levels in kidney were measured by reverse-phase high performance liquid chromatography-electrospray ionization-tandem mass

spectrometry technique, as described in precedent studies.[38,39]

Migration Assay

Elicited peritoneal macrophages were harvested from PAFR-KO and PAFR-WT mice 3 days after injection of 4% thioglycolate. Peritoneal exudate cells were washed with phosphate-buffered saline and resuspended in RPMI 1640 medium supplemented with 0.1% bovine serum albumin. Cell migration was evaluated using a 96-well Boyden chamber as described previously, with minor modifications.[40] The PAF at concentrations of 0, 1, and 10 nmol/L in 300 μl of RPMI 1640 containing 0.1% bovine serum albumin was added to the lower wells of a chemotaxis chamber (Neuro Probe, Inc., Gaithersburg, MD). A polycarbonate filter (8-μm-pore size; Neuro Probe, Inc.) was layered onto the wells; 65 μl of cell suspension (4.0×10^6/ml) were applied to the upper wells. The chamber was incubated at 37°C in a humidified atmosphere in the presence of 5% CO_2 for 2 hours. At the end of incubation, the filter was removed, fixed with methanol, and stained with Diff-Quick (Sysmex Corp., Hyogo, Japan). Cells on the upper side of the filter were wiped away. The number of cells that had migrated to the lower side was determined by measuring optical densities at 595 nm using a 96-well microplate reader (model 3550; Bio-Rad Laboratories Inc., Hercules, CA). Each experiment was performed in triplicate.

Statistical Analysis

Results of statistical analyses are expressed as means ± SEM. Differences among groups at the same time point were examined using Student's *t*-test. Differences among experimental groups at different time point were confirmed by one-way analysis of variance followed by the Tukey-Kramer test for individual comparison of group means. These calculations were performed using StatView-J5.0 (SAS Institute Inc., Cary, NC). The null hypothesis was rejected when P was <0.05.

Results

Attenuation of Renal Dysfunction in PAFR-KO Mice and Efficacy of PAFR Antagonist

Administration of FA with sodium bicarbonate induced transient elevation of BUN and Cr at 48 hours after injection followed by subsequent renal dysfunction accompanied with interstitial fibrosis. Basal levels of BUN and Cr in PAFR-WT and PAFR-KO mice were similar [PAFR-WT: BUN 28.1 ± 0.8 mg/dl, Cr 0.25 ± 0.01 mg/dl (n = 16) versus PAFR-KO: BUN 27.8 ± 0.9 mg/dl, Cr 0.24 ± 0.01 mg/dl (n = 16)]. The measurement at 48 hours after FA injection showed statistically significant elevation of BUN and Cr compared with baseline in both PAFR-WT and PAFR-KO mice (PAFR-WT, $P < 0.001$; PAFR-KO, $P < 0.005$), and the levels of

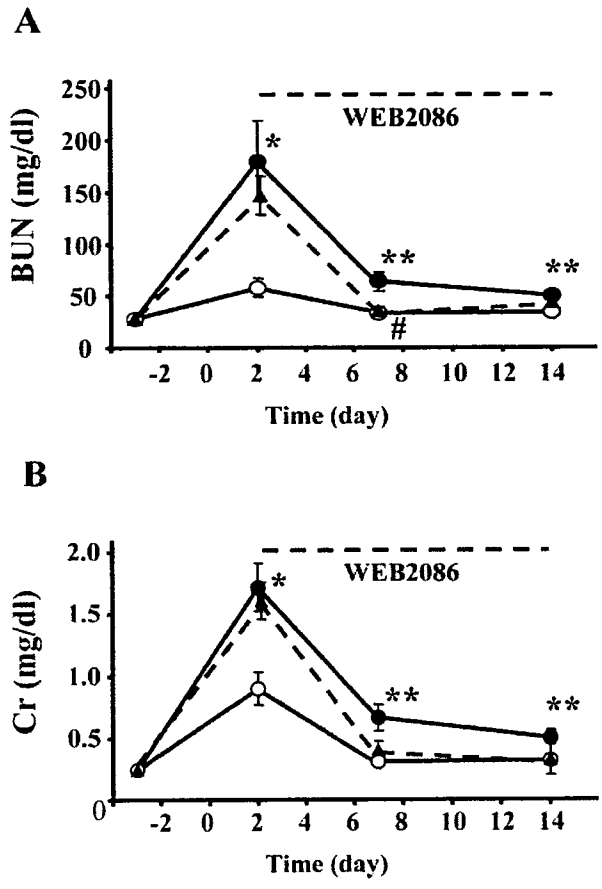

Figure 1. Time course of BUN (**A**) and Cr (**B**) levels in PAFR-KO and PAFR-WT mice subjected to FA administration. **Filled circles** indicate PAFR-WT mice, **open circles** indicate PAFR-KO mice, and **filled triangles** indicate WEB2086-treated PAFR-WT mice. WEB2086 was injected every day from days 2 to 14. The numbers of animals were 16 at days −3 and 2, 8 at days 7 and 14 in PAFR-WT and PAFR-KO mice, and 5 in WEB2086-treated PAFR-WT mice. $^*P < 0.005$, $^{**}P < 0.05$ (PAFR-WT versus PAFR-KO). $^{\#}P < 0.05$ (PAFR-WT versus WEB2086-treated PAFR-WT).

BUN and Cr in PAFR-WT mice were significantly higher compared with levels in PAFR-KO mice [PAFR-WT: BUN 180.0 ± 39.0 mg/dl, Cr 1.71 ± 0.20 mg/dl (n = 16) versus PAFR-KO: BUN 58.2 ± 8.9 mg/dl, Cr 0.90 ± 0.13 mg/dl (n = 16); $P < 0.005$] (Figure 1). The significant differences were also valid at days 7 and 14 [PAFR-WT: BUN 63.7 ± 9.4 mg/dl, Cr 0.66 ± 0.11 mg/dl (n = 8) versus PAFR-KO: BUN 33.1 ± 3.3 mg/dl, Cr 0.31 ± 0.04 mg/dl (n = 8); $P < 0.05$, at day 7] [PAFR-WT: BUN 50.2 ± 5.2 mg/dl, Cr 0.50 ± 0.06 mg/dl (n = 8) versus PAFR-KO: BUN 33.8 ± 3.3 mg/dl, Cr 0.31 ± 0.04 mg/dl (n = 8); $P < 0.05$, at day 14]. Treatment with WEB2086 after acute phase from day 2 to day 14 also showed partial protective effects for renal dysfunction [day 2: BUN 146.9 ± 18.7 mg/dl, Cr 1.60 ± 0.15 mg/dl; day 7: BUN 35.5 ± 3.6 mg/dl, Cr 0.39 ± 0.07 mg/dl; day 14: BUN 43.4 ± 3.9 mg/dl, Cr 0.32 ± 0.12 mg/dl (n = 5)]. In addition, there was a significant difference between WEB2086-treated and untreated PAFR-WT mice in BUN level at day 7 ($P < 0.05$) (Figure 1).

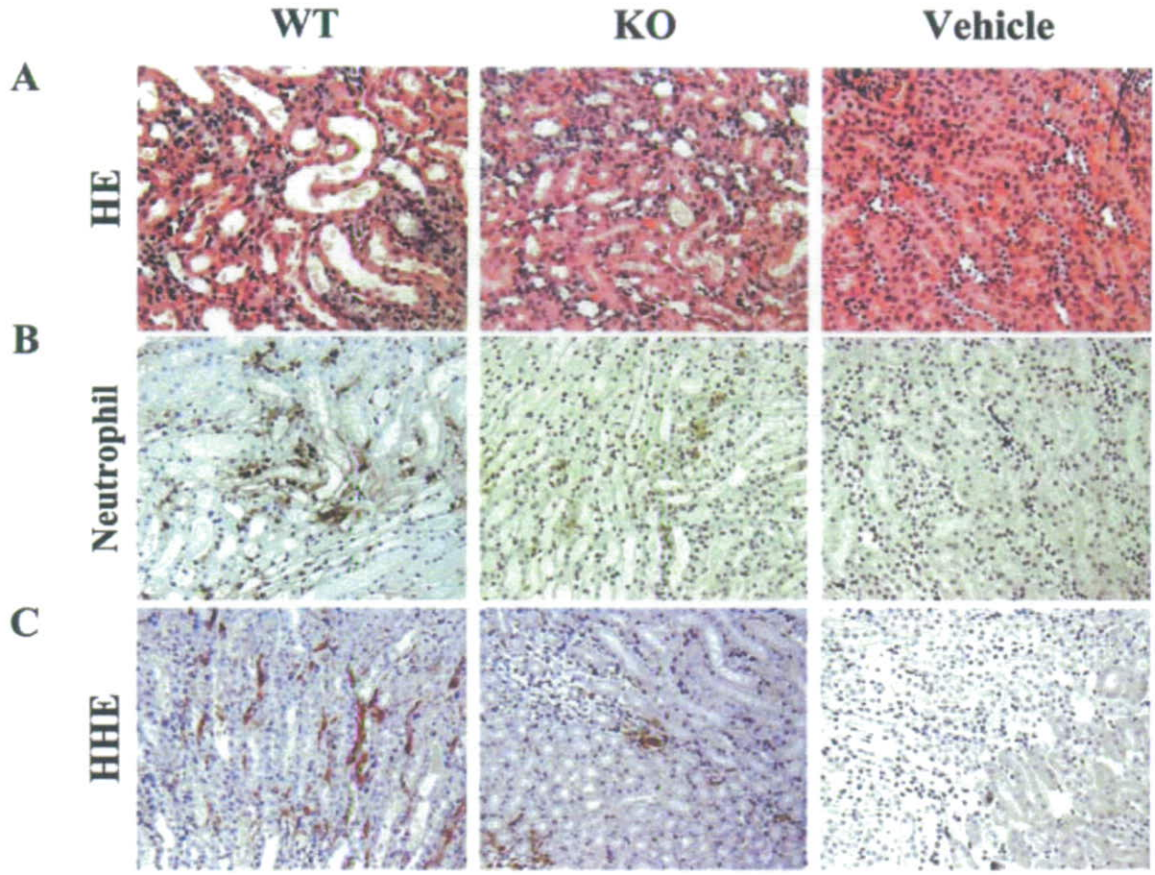

Figure 2. Histological findings at day 2 stained with H&E (**A**), immunohistochemistry using antibody to neutrophil (**B**), and antibody to HHE-modified proteins (**C**). Vehicle-treated PAFR-KO and PAFR-WT showed identical results. Therefore, only PAFR-WT mice are shown. Original magnifications, ×200.

Neutrophil and ROS Production in Acute Tubular Damage

In addition to attenuation of renal dysfunction, morphological analyses demonstrated that acute tubular necrosis was significantly milder in PAFR-KO mice than in PAFR-WT mice at 48 hours after FA administration (Figure 2A). Immunohistochemical staining with anti-neutrophil antibody showed that infiltrating neutrophils decreased significantly in PAFR-KO mice compared with PAFR-WT mice at day 2 [PAFR-WT: 27.5 ± 2.3/×200 field (n = 4) versus PAFR-KO: 6.9 ± 1.0/×200 field (n = 4); $P <$ 0.001] and were detected predominantly around the damaged tubules (Figure 2B and Figure 3).

Through propagation of lipid peroxidation, ROS will damage tissue. Antibody to HHE, produced in the peroxidative metabolism of ω-3 polyunsaturated fatty acids in cell membranes, is a specific marker to detect lipid peroxidation.[35] Immunohistochemical analyses dominantly detected HHE-modified proteins around peritubular capillaries of damaged kidney tissues (Figure 2C). Lipid peroxidation was also quantified in kidney homogenates by Western blot analysis. In PAFR-WT mice, kidney homogenates showed a higher intensity of immunoreactive bands of HHE-modified proteins compared with those from PAFR-KO mice (Figure 4).

To evaluate the contribution of neutrophils for acute phase of FA-induced renal injury at day 2, we also injected FA into PAFR-WT mice pretreated with neutrophil depletion antibody. Neutrophil depletion was confirmed through flow cytometry analyses (Figure 5A). These ani-

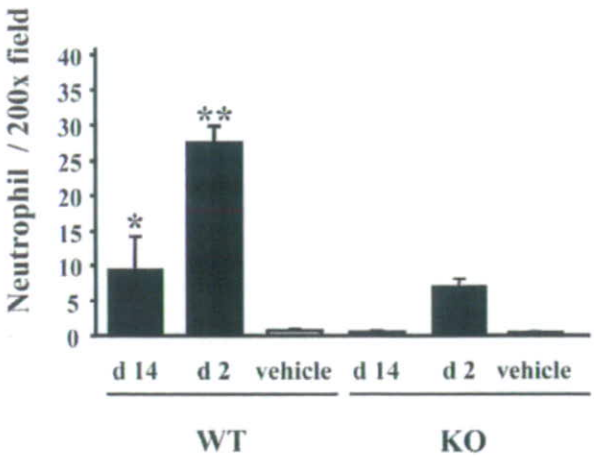

Figure 3. Number of infiltrating neutrophils in FA-injured kidney. Five animals were in the FA group; four received the vehicle. *$P <$ 0.005 versus PAFR-KO mice at day 14 (d 14). **$P <$ 0.00005 versus PAFR-KO mice at day 2 (d 2).

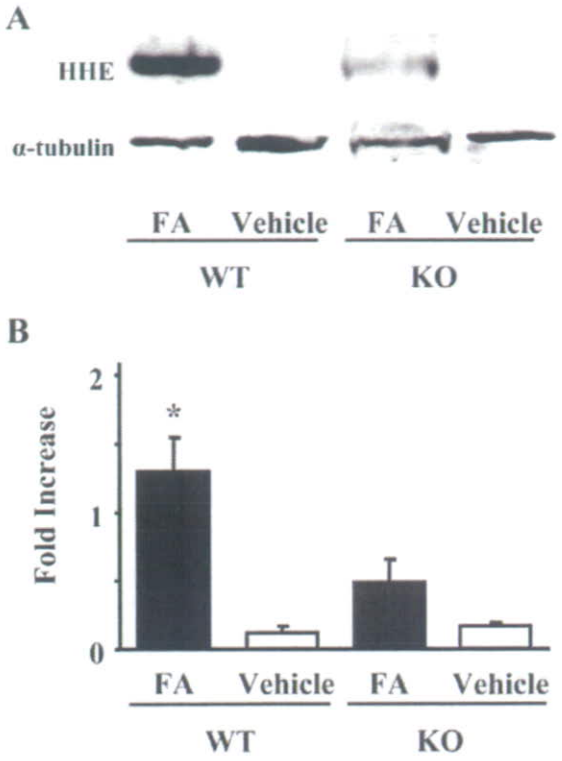

Figure 4. Western blot analysis of HHE-modified protein expression in kidney homogenates at day 2. A representative image is shown in **A** (**top**). **B:** The histogram depicts the relative density of bands in comparison with α-tubulin. Five animals were in the FA group; three received the vehicle. $^*P < 0.05$ versus PAFR-KO mice with FA administration.

mals showed remarkable amelioration of renal dysfunction [control: BUN 133.5 ± 21.1 mg/dl, Cr 1.54 ± 0.09 mg/dl (n = 5) versus neutrophil depletion: BUN 35.3 ± 2.4 mg/dl, Cr 0.47 ± 0.16 mg/dl (n = 5); $P < 0.005$] (Figure 5, B and C).

Development of Interstitial Fibrosis and Macrophage Infiltration

The FA-induced renal injury model showed development of segmental interstitial fibrotic lesions at day 14. Figure 6A shows that interstitial fibrotic areas stained in blue by Masson's trichrome staining were more prominent in kidneys of PAFR-WT mice than in those of PAFR-KO mice. Quantitative analyses demonstrated that the fibrotic area in PAFR-WT mice was significantly larger than PAFR-KO mice [PAFR-WT: 5.4 ± 0.7% (n = 5) versus PAFR-KO: 2.1 ± 0.7% (n = 5); $P < 0.05$] (Figure 7). Immunohistochemical and Western blot analyses with anti-α-SMA antibody were performed to detect interstitial myofibroblasts. Positive staining of α-SMA was found in the identical site of fibrotic area stained blue with Masson's trichrome staining (Figure 6B) and seen in vascular smooth muscle cells (data not shown). Kidney homogenates of PAFR-WT mice were shown by Western blot analysis to have a higher intensity of immunoreactive bands of α-SMA than those from PAFR-KO mice (Figure 8).

Macrophage infiltration was evaluated using immunostaining for F4/80, a specific macrophage antigen. Infiltrated F4/80-positive macrophages were detected in the peritubular interstitium around fibrotic areas in kidneys harvested 14 days after FA administration (Figure 6C). The number of infiltrated F4/80-positive macrophages at

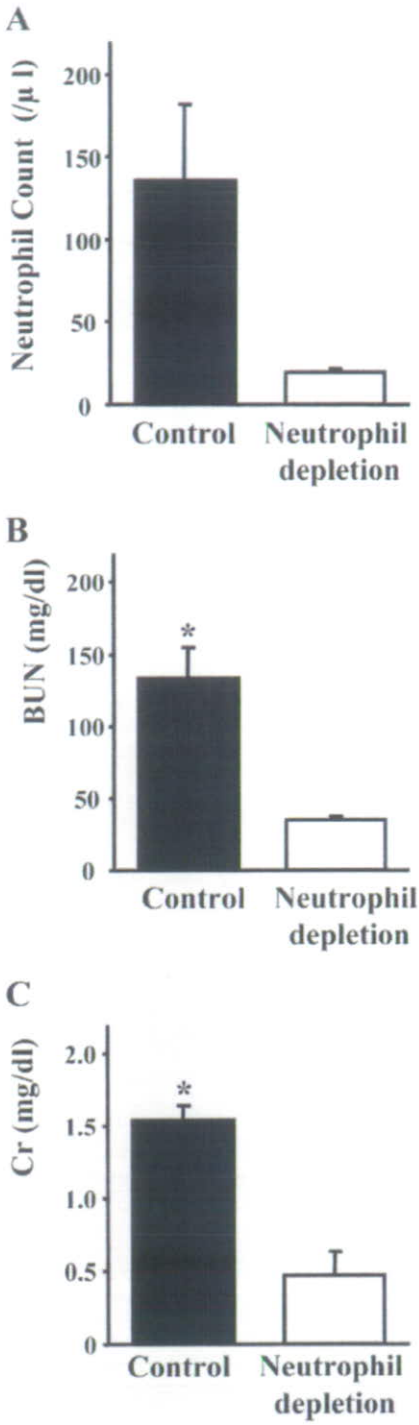

Figure 5. Effects of neutrophil depletion on acute phase of FA-induced renal injury. Injection of a monoclonal neutrophil depletion antibody (RB6-8C5) at day −1 caused a significant decrease of neutrophil count in blood of PAFR-WT mice at day 2. **A:** Renal dysfunction at day 2 was attenuated with treated PAFR-WT mice compared with untreated PAFR-WT mice (**B** and **C**). $^*P < 0.005$ versus untreated PAFR-WT mice. Five animals were in each group.

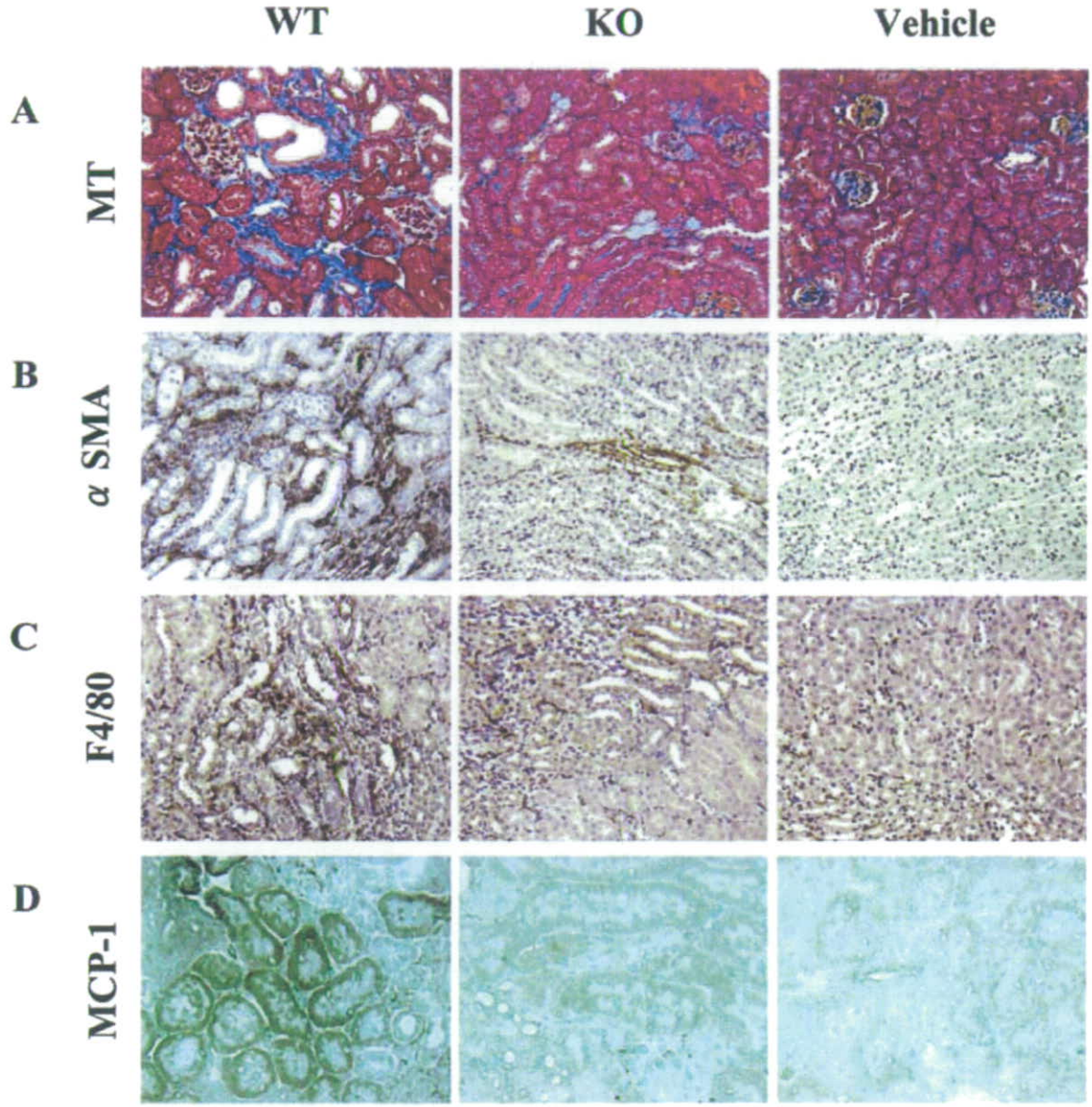

Figure 6. Histological findings at day 14 stained with Masson's trichrome (**A**), immunohistochemistry using antibody to α-SMA (**B**), antibody to F4/80-positive macrophage (**C**), and immunohistochemical analyses using antibody to MCP-1 with frozen sections. Vehicle-treated PAFR-KO and PAFR-WT showed identical results. Therefore, only PAFR-WT mice results are shown. Original magnifications: ×100 (**A**); ×200 (**B**, **C**); ×400 (**D**).

day 14 in PAFR-WT mice was significantly higher than that in PAFR-KO mice [PAFR-WT: 97.5 ± 11.9/×200 field (n = 5) vs. PAFR-KO: 32.1 ± 8.6/×200 field (n = 5); $P <$ 0.05] (Figure 9). In contrast, the numbers of F4/80-positive cells in kidneys harvested at 48 hours after FA administration did not differ among groups [PAFR-WT: 28.5 ± 6.7/×200 field (n = 5) versus PAFR-KO: 18.7 ± 2.0/×200 field (n = 5); P = 0.21].

The PAFR-WT mice treated with WEB2086 after acute phase every day (from day 2 to day 14) showed significantly decreased interstitial fibrosis and macrophage infiltration at day 14 compared with untreated PAFR-WT mice [fibrotic area: 3.5 ± 0.3% (n = 5); $P < 0.05$ versus untreated PAFR-WT mice and macrophage counts: 66.0 ± 6.3/×200 field (n = 5); $P < 0.05$ versus untreated PAFR-WT mice] (Figures 7 and 9).

TNF-α and MCP-1 Expression in FA-Induced Renal Injury

We examined TNF-α and MCP-1 mRNA expression using TaqMan real-time PCR assay to confirm the contribution of macrophages for FA-induced renal injury. Decreased expression of both TNF-α and MCP-1 were shown in the kidney of PAFR-KO mice compared with PAFR-WT mice (Figure 10). Furthermore, increased expression of these cytokines at day 14 was found only in PAFR-WT mice.

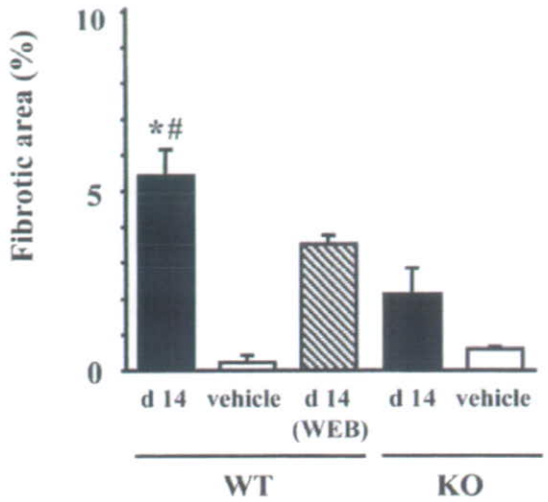

Figure 7. The fibrotic area in the cortex from the kidney at day 14 (d 14) was calculated using a computer-aided evaluation program. Five animals were in the FA group; four received the vehicle. $^{*}P < 0.05$ versus PAFR-KO mice. $^{\#}P < 0.05$ versus PAFR-KO mice with FA administration. $^{*}P < 0.05$ versus WEB2086-treated PAFR-WT mice.

These results indicate that macrophage accumulation to the injured kidney was amplified even after acute tubular damage at day 2. In addition, immunohistochemical analysis at day 14 revealed that MCP-1 protein was expressed dominantly in the proximal tubular epithelium (Figure 6D).

PAF Levels in Kidney

To clarify the presence of PAF and PAFR pathway in FA-induced renal injury, we examined the levels of PAF in the kidney. The renal PAF levels were virtually the same in normal kidney of PAFR-KO and PAFR-WT mice [PAFR-WT: 0.96 ± 0.15 pg/mg tissue (n = 4) versus PAFR-KO: 1.16 ± 0.39 pg/mg tissue (n = 4)] and increased by administration of FA, especially at day 14 in PAFR-WT mice [PAFR-WT at day 14, 11.08 ± 3.38 pg/mg tissue (n = 4) versus PAFR-WT normal kidney; $P < 0.05$] (Figure 11). The PAF levels in PAFR-WT mice were higher than those in PAFR-KO mice, especially at day 14, but those differences were not statistically significant.

PAF-Induced Chemotaxis in Macrophage

Infiltration of F4/80-positive macrophages in interstitial fibrosis of the kidney was attenuated in PAFR-KO mice; PAF is also known as a potent chemoattractant for leukocytes. For that reason, we examined the direct chemotactic activity of macrophages to PAF using a Boyden chamber system. Macrophages isolated from PAFR-WT mice showed a remarkable chemotactic activity to PAF at concentrations of 1 and 10 nmol/L. On the other hand, PAF induced no chemotaxis in macrophages isolated from PAFR-KO mice (Figure 12).

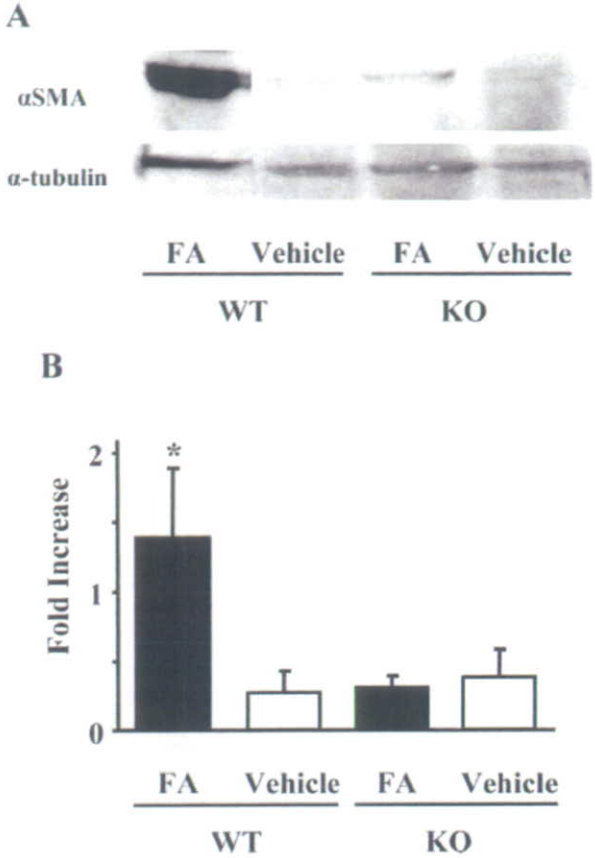

Figure 8. Western blot analysis of α-SMA expression in kidney homogenates at day 14. A representative image is depicted in **A** (**top**). **B:** The histogram illustrates the relative density of bands in comparison with α-tubulin. Five animals were in the FA group; four received the vehicle. $^{*}P < 0.05$ versus PAFR-KO mice with FA administration.

Discussion

This study demonstrated that FA-induced renal injury comprises an acute and a subsequent chronic phase. Infiltration of ROS-producing neutrophils in acute tubular damage and macrophages in chronic interstitial fibrosis was attenuated significantly in PAFR-KO mice in comparison with PAFR-WT mice. Moreover, treatments of PAFR-WT mice with neutrophil depletion antibody and PAFR antagonist, which were started after the acute phase, also showed significant amelioration of acute tubular damage and macrophage infiltration and interstitial fibrosis in the chronic phase. Therefore, our data indicate that leukocytes play a crucial role both in the acute phase and the chronic phase of this animal model and that PAF is involved in pathogenesis of FA-induced inflammatory renal injury. To our knowledge, this study is the first to demonstrate the attenuation of renal injury in PAFR-KO mice, although several precedent studies have shown the effects of PAFR antagonists on renal disease in animal models.[10–12] However, those studies using PAFR antagonists often include problems related to drug specificity. Some PAFR antagonists inhibit the effect of histamine through interaction with its G protein-coupled receptor[13,15]; other antagonists inhibit the activity of PAF

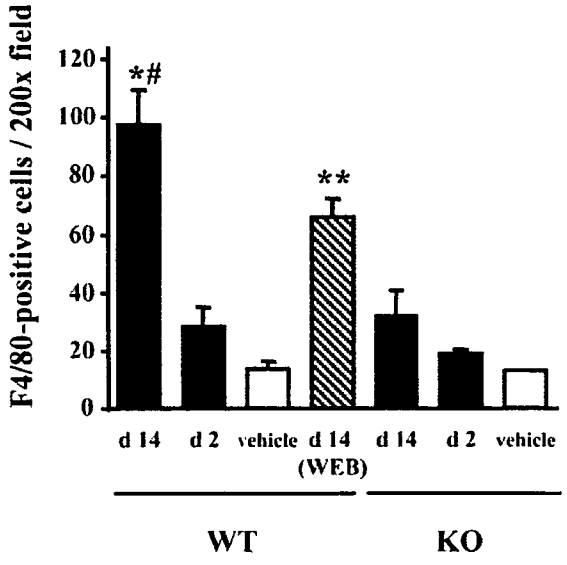

Figure 9. Number of infiltrating F4/80-positive cells in the tubulointerstitium with FA-induced renal injury. Five animals were in the FA group; four received the vehicle. $^{*}P < 0.005$ versus PAFR-KO mice at day 14 (d 14). $^{\#}P < 0.05$ versus WEB2086-treated PAFR-WT mice at day 14. $^{**}P < 0.05$ versus PAFR-WT mice at day 14.

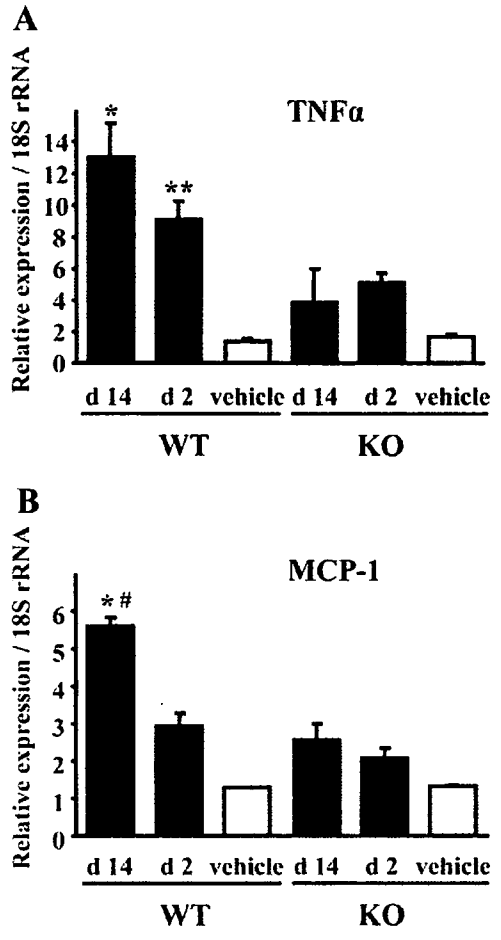

Figure 10. Quantitative analyses of expression of TNF-α (**A**) and MCP-1 (**B**) using real-time PCR. Eight animals were in the FA group; three received the vehicle. **A:** TNF-α expression was higher in PAFR-WT mice, both at days 2 and 14. $^{*}P < 0.005$ versus PAFR-KO mice at day 14 (d 14), $^{**}P < 0.05$ versus PAFR-KO mice at day 2 (d 2). **B:** MCP-1 expression was higher in PAFR-WT mice than in PAFR-KO mice at day 14. $^{*}P < 0.05$ versus PAFR-KO mice at day 14. Moreover, MCP-1 expression increased in PAFR-WT mice at day 14 greater than that at day 2. $^{\#}P < 0.05$ versus PAFR-WT mice at day 2.

acetylhydrolase, which inactivates PAF.[14,16] The present study demonstrates the pathological role of PAF in FA-induced renal injury using genetically engineered mice in which PAFR signaling was decreased congenitally by disrupting the PAFR gene. Several reports have used PAFR-KO mice to elucidate the role of PAF in various pathophysiologies. The PAFR-KO mice exhibited attenuation in animal models in which inflammatory injuries were crucial: chemical lung injury,[18] bronchial asthma,[19] and sponge-induced subcutaneous granuloma formation.[20] On the other hand, PAFR-KO mice showed exacerbation of infection models such as pulmonary gram-negative bacteria infection[41] and cardiac *Trypanosoma* infection.[42] Those reports, along with the present study, indicate that PAF causes both beneficial and deleterious effects by activating leukocytes in different circumstances.

The neutrophil infiltration and lipid peroxidation of HHE in kidney at day 2 in PAFR-KO mice were significantly lower than those of PAFR-WT mice in this study. Stimulation of neutrophils with PAF *in vitro* engenders numerous cellular responses including chemotaxis,[43–45] degranulation,[46] and ROS production.[43,47] Priming neutrophils with PAF enhances ROS production by NADPH oxidase, which catalyzes superoxide production.[48] Through *in vivo* analysis with ischemia-reperfusion kidney injury, Kelly and colleagues[49] showed that PAFR antagonist reduced neutrophil infiltration. Lloberas and colleagues[50] showed that antioxidant treatment with vitamin C decreased PAF release from kidney and neutrophil infiltration to kidney. Moreover, neutrophil depletion by a monoclonal antibody RB6-8C5 significantly ameliorated FA-induced acute tubular damage in this study. These findings indicate that ROS produced by activated infiltrating neutrophils play an important role in FA-induced acute tubular damage. On the other hand, incomplete recovery of FA-induced renal injury in PAFR-KO mice and better improvement in neutrophil-depleted PAFR-WT mice than PAFR-KO mice, despite the lack of statistical difference between them, indicates that additional factors related to neutrophil activation might contribute to FA-induced injury.

Recruitment and activation of macrophages and lymphocytes to the kidney play a central role in a final pathway of most injuries to chronic kidney damage. Therefore, regulating these immunocompetent cells might be a potential target for therapeutic intervention for kidney disease.[4] The PAFR-KO mice showed significant amelioration of FA-induced renal injury that developed to remarkable interstitial fibrosis with macrophage infiltration accompanied by the increase in the expression of TNF-α and MCP-1. Contribution of TNF-α for interstitial fibrosis was demonstrated in unilateral ureter obstruction, another renal fibrosis model, with TNF-α receptor knockout mice.[51] In PAFR-KO mice, reduced macrophage infiltration number and lack of a PAF receptor pathway might engender decreased TNF-α expression in the kidney and